Performance Evaluation of Next Generation Wireless UAV Relay with Millimeter-Wave in Access and Backhaul

A thesis submitted in fulfilment the requirements for the degree of

Master of Engineering

Shah Khalid Khan

B.Eng.

University of Engineering and Technology, Peshawar

School of Engineering
College of Science, Engineering and Health
RMIT University

Sep, 2019

Declaration

I certify that except where due acknowledgment has been made, the work is that of the author alone; the work has not been submitted previously, in whole or in part, to qualify for any other academic award; the content of the thesis is the result of work which has been carried out since the official commencement date of the approved research program; any editorial work, paid or unpaid, carried out by a third party is acknowledged; and, ethics procedures and guidelines have been followed.

I would like to acknowledge the Australian Government for Research Training Program (RTP) Fees Offset Scholarship.

Shah Khalid Khan

Sep 2019

Dedication

This dissertation is dedicated to My Parents, who instilled in me the virtues of perseverance and commitment and relentlessly encouraged me to strive for excellence.

Acknowledgements

Pursuing Master by Research degree is both challenging and exciting experience. It's just like climbing a high mountain, step by step, accompanied with bitterness, encouragement with help of many kind people. And, in my case, they are my supervisors, Dr. Karina Gomez Chavez and Dr. Akram Al-Hourani.

First of all, I would like to express my profound gratitude to Dr. Karina Gomez Chavez and Dr. Akram Al-Hourani for giving me the opportunity to pursue this Master by Research degree, during which they provided excellent research atmosphere and technical support. I also would like to thank them for their patience, guidance, care, and for their experience that considerably added to my research skills. I would like to acknowledge my colleagues Usman Naseem, Haris Siraj and Muhammad Shehram Shah Syed for their careful reading and feedback on my thesis.

Finally, I thank RMIT University for having provided me with 2 years of a challenging yet rewarding Master by Research experience especially the HDR administration team within the School of Engineering for their assistance and support during my candidature.

I would like to acknowledge the Australian Government for Research Training Program (RTP) Fees Offset Scholarship.

Abstract

Future wireless communication, particularly densified 5G networks, will bring numerous innovations to the telecommunication industry and will support 100-fold gain in throughput rates, 100-fold in capacity (for at least 100 billion devices), individual user data rate of up-to 10 Gb/s, extremely low latency and response times. In such a scenario, the use of Unmanned Aerial Vehicle (UAV) as a Base Station (gNB) becomes a viable option for providing 5G services, both on-demand and on a regular basis. Recent development of UAVs have made its deployment faster and reliable, resulting in a shift in its usage from traditional military to more commercial and corporate industries. On the other hand, due to the abundant availability of bandwidth in the millimeter-wave band (mmWave), there is an immense potential to utilize this band for next generation radio systems. In this case, smart integration of UAVs in 5G network provides immense potential, however, such network require efficient placement mechanism for providing blazingly fast wireless cellular network services.

In this study, we analyze and describe the distinctive characteristics of mmWave propagation. The main goal is to investigate and evaluate the use of mmWave in Access and Back-haul communication links simultaneously for Amplify-and-Forward relays deployed on UAVs. We formulate the required mathematical framework for calculating the UE received power for direct path (gNB-UE) and relay path (gNB-UAV-UE) based on two cases; (i) Friis Transmission Equation and (ii) Log-Distance Path loss Model. We conduct simulations using ray-tracing simulator in different scenarios while comparing and verifying the simulation results vs mathematical equations. For the proposed system architecture, International Telecommunication Union (ITU) recommendation city model is used to calculate the probability for Line of Sight (LoS) and Non Line of Sight (NLoS) paths in different urban environments. Furthermore, we study and identify different parameters i.e., UAV location, and amplification factor to maximize the performance of an Amplify-and-Forward UAV based relay for providing enhanced coverage to the users. Similarly, the optimum UAV-gNB height is evaluated in different urban environments while providing coverage to the users via an Amplify-and-Forward relay. The study concludes with the Signal to Noise Ratio (SNR) analysis for the relay path compared with the direct path where we identify the constraints for effective relaying.

Contents

List of Figures

List of Tables

Chapter 1

Introduction

This chapter provides the motivation and main objectives of this study. We start with describing next generation wireless networks focusing particularly on 5G telecommunication networks, and study the effectiveness of UAV-gNB in cellular networks and the potential of mmWave band in future telecommunication networks. Then, we continue by describing the research problem, stating the research objectives and the main research questions. Later on, we explain the research methodology, summarize the steps required to accomplish the aims of this study. At the end of this chapter, the organization of the thesis is described, providing highlights on the subsequent chapters.

1.1 Motivations and Challenges

Radio communication has undergone several generational evolutions in the last 40 years. Each generation of cellular technology roughly lasted a decade or so, before being rendered obsolete through innovations in communication technologies. The first generation of telecommunication networks (1G) commonly known as the voice era provided telephone services to masses. Mostly based on wired architecture, this was the longest reigning generation of telecommunication networks. The proliferation of telephony services in everyday life led to the development of the second generation of communication systems (2G), which introduced the concept of digital mobile telecommunication through wireless networks and portable devices. The 2G technology went through continuous enhancements ushering in the data/Internet era mostly known as 2.5/3G/4G-LTE generations. These generations continues to be in operation until the first decade of the new millennium. The advancement in information technology has led to the development of revolutionizing technologies such as Internet of Things (IoT) which envisions inter-connectivity of everyday devices such as cars, mobile phones, and home appliances etc. This has created the ever expanding need for scalable, resilience and ubiquitous telecommunication networks capa-

ble of supporting extremely high data rates with low latency. The latest generation of radio communication has been referred to as 5G [6]. It is envisioned that 5G will transform existing service architecture and will provide a singular network slice (instead of differentiating between voice and data services) to the users. 5G services, Release-16 expected to be standardized by 2020 [7], however, 3GPP Release 15-the first full set of 5G standards is released in 2019 [6]. 5G Services will be capable of providing Cellular Access part to support traffic up-to 10 Gbps with sub-millisecond latency. The super connected era of 5G systems is anticipated to provide wireless services for evolving applications such as augmented reality, virtual reality traffic, and streaming of millions of minutes of video content per second. Cisco, a leading telecom systems company, predicts that in 2021 the demand for mobile data rate will be twice as much as the demand for fixed line data services [8]. 5G networks are based on much wider spectrum allocations in the yet untapped mmWave frequency band, allowing for higher data rates and highly efficient (pencil beam forming) antennas at both the mobile devices and base stations [9].

The two most promising benefits of mmWave are: (i) wider bandwidth availability between 30 and 300 GHz which is 200 times larger spectrum when compared with the current cellular networks [9; 10], (ii) can generate beam-forming with very high gain due to multiple antenna systems, which can offer a transmission range that exceeds 130m [11] and in some specific scenarios coverage can be reached up-to 200m [12]. Nevertheless, the critical challenges of using mmWave in wireless cellular networks are propagation loss and sensitivity to blockage as highlighted in Fig 1.1.

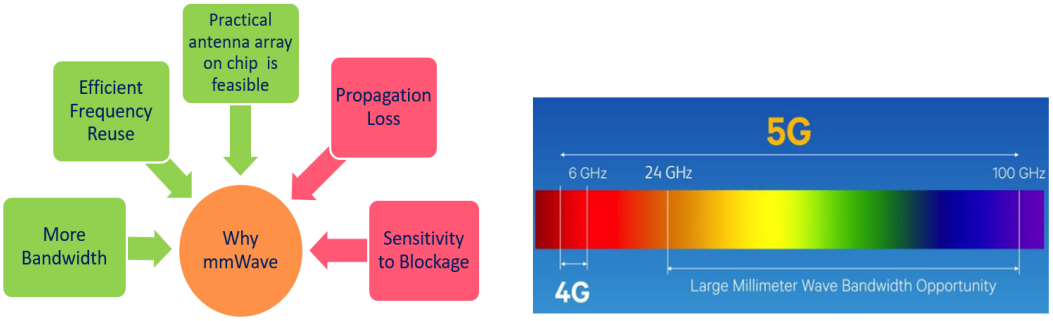

(a) Benefits and challenges in mmWave band

(b) mmWave frequency band

Figure 1.1: Benefits and challenges in mmWave.

The potential of utilizing UAVs as a relay gNB in cellular communication is a topic of interest for academia and telcos alike [13; 14]. Modernization and innovation in UAV research and applications have resulted unwrapping of new avenues of utilization, especially its unparalleled scalibility and resilience in deployment of on the go and pseudo permanent cellular communication systems. The main reasons are; the reliable LoS aerial-to-ground links, and the maneuverability in three-dimensional (3D) space. UAVs are getting recognition in the two main scenarios: (i) re-establishing communications shortly after a disaster and (ii) enhancing network capacity during

high demand scenarios (sports events, concerts and political/social activities) [15; 16; 17]. The use of UAVs in telecommunication networks is governed by supervision in two areas: (i) aviation regulations regarding the operation of UAVs and (ii) technological issues regarding UAV based telecom networks. In both of these domains, there are some major aspects which require in-depth study; these include UAV channel modelling, UAV deployment, cellular network planning for UAVs based networks, radio resource management, energy efficiency and UAV trajectory optimization [18; 19; 20; 21]. This study focuses on using UAV-gNB as an Amplify-and-Forward relay.

The main applications of UAV based gNB includes:

- To provide UE's signals for acceptable network, especially in shadowed zones,
- To increase data rates or densifying an existing network.

The promising benefits of UAV supported gNB are:

- LoS aerial-to-ground link, and
- Controllable movement in three-dimensional (3D) space.

However, the main challenges associated with mmWave band are:

- UAV channel modelling,
- Resource management algorithms,
- Energy efficiency,
- Trajectory optimization
- Optimum placement of UAV-gNB for enhancing cellular coverage.

The above points are depicted in Fig. 1.2

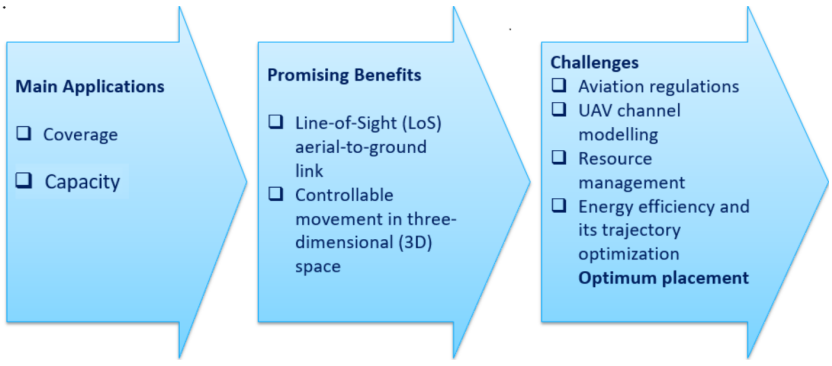

Figure 1.2: UAV based gNB application and challenges.

1.2 Research Problem and Objectives

The mmWave band is capable of overcoming the scarcity of bandwidth in future wireless communications systems [22]. The mmWave has been implemented in many scenarios for Access or Backhaul communication, but its capability in using it simultaneously for both Access and Backhaul link is an open research area and still needs to be explored [20; 23]. Moreover, the other challenges which are not yet studied include the practical evaluation of scenarios focusing on fulfilling user demand of high data rates and cellular mobile industry standards. The main challenge in the uptake of mmWave is its intrinsically high path loss with regards to the growing distance from transmitter to receiver, the second challenge is its sensitivity to blockages. This band can only be utilized if these technical issues are overcome, therefore, an in-depth study and analysis is required to develop additional architectures that overcome these constraints. In this study, we present the results of our evaluation of a 5G-network architecture which uses UAVs as an Amplify-and-Forward relay as shown in Fig 1.3.

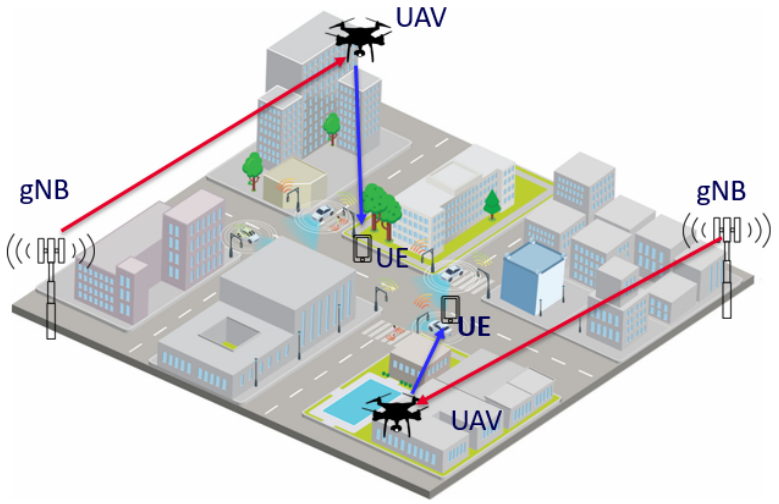

Figure 1.3: Network model of UAV relay network in the context of 5G.

The main objectives of this study are:

- To provide an end-to-end channel model which is capable of supporting the dynamics of 5G networks based on Amplify-and-Forward UAV relays in the mmWawe band.
- To determine the optimum Amplify-and-Forward UAV relay height for coverage maximization in randomly distributed users scenarios.
- To compare the performance of the direct path (between the gNB and UE) with respect to the relay path (between the gNB and UE via UAV).

1.3 Research Questions

Based on the previous discussion, especially the research objectives, we formulate the research questions as below.

- **RQ1: What are the fundamental parameters for the development of a mathematical framework capturing the link performance of an Amplify-and-Forward UAV relay using mmWave at the Backhaul and the Access link?**
  (Discussed in Chapter 3)
  Mathematical modelling is the key to understand wireless signal propagation characteristics. This model is instrumental to the identification of important parameters that need to be optimized for improving service quality. The following objectives address RQ1:
  - To formulate a mathematical framework for calculating UE received power for the direct path (gNB-UE) and the relay path (gNB-UAV-UE). The proposed framework is to be based on the Friis Transmission Equation and Log-Distance Path loss Model.
  - To utilize the probability for LoS and NLoS paths in different urban environments for the proposed system architecture using ITU recommended city model,
  - To perform SNR analysis of the relay path in comparison with the direct path,
  - To identify the constraint i.e., value of amplification factor that influence the effectiveness of relay path over direct path.
- **RQ2: What is the expected performance of an Amplify-and-Forward UAV relay for providing coverage to the UEs? What is impact on the UAV-gNB optimum height, while providing coverage to the UEs in different urban environments?**
  (Explained in Chapter 4)
  We evaluate the mathematical framework against simulated results. Ray-tracing simulation is a method for studying simulation propagation and having significant capability in evaluating channel characteristics. This method is very useful for evaluating novel radio technologies. The following objectives address RQ2:
  - To implement the mathematical framework in a simulator using ray-tracing method,
  - To compare and verify the simulation results versus the mathematical framework,
  - Evaluation of UAV-gNB optimum height, while providing coverage to the UEs in different urban environments,
  - To perform numerical analysis of the SNR for the relay path in comparison with the direct path,

– Evaluation of the received power in relay paths in comparison with the direct path, while keeping variant amplification factor.

1.4 Methodology

This section describes the steps and the processes needed to address the research questions and to achieve the objectives presented in the previous section. Fig. 1.4 provides a graphical illustration of the steps and methods undertaken to conduct this study:

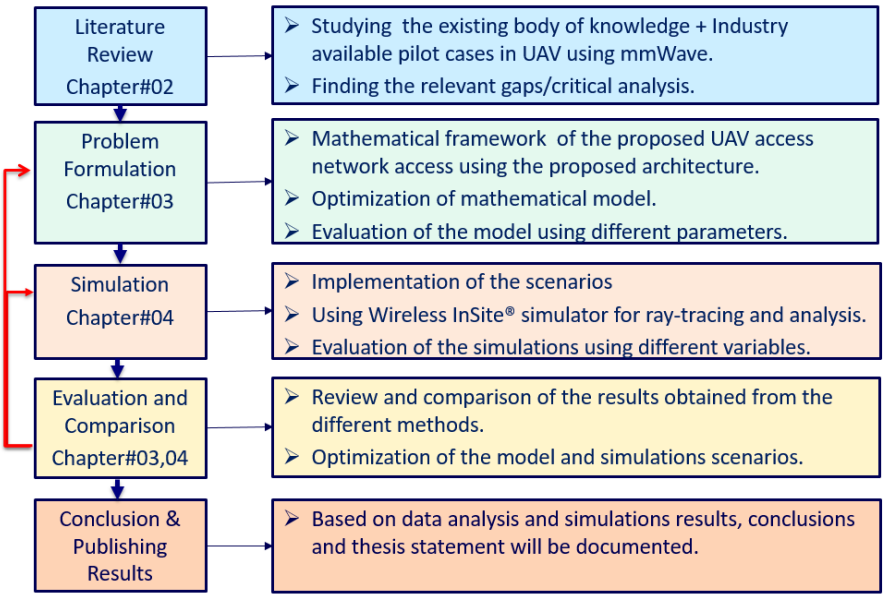

Figure 1.4: Research methodology for achieving research objectives.

Below is the brief explanation of the steps highlighted in Fig. 1.4.

1. **Literature Review:** Literature Review provides a consolidated summary of an in-depth analysis of works published by prominent researchers. The two main areas study and explored in literature review are; (i) study of various mmWave propagation characteristics, path loss models models, and (ii) the use of UAVs as an Amplify-and-Forward relay base stations as well as suitable architectures. The review identifies relevant gaps in this domain and provides a critical analysis which form the foundations of research questions and objectives of this study.

2. **Problem Formulation and Mathematical Modelling:** Mathematical framework is formulated using the proposed Amplify-and-Forward UAV relay architecture. We used (i) Friis Transmission Equations, and (ii) mmWave path loss models for formulating the end-to-end equation of an Amplify-and-Forward UAV relay network.

3. **Ray-Tracing Simulations:** In this phase, Wireless InSite ray-tracing simulator is used for

ray-tracing simulation and analysis of the proposed scenarios. We also evaluate, analyze and explain direct path and relay paths using LoS and NLoS scenarios. We use ITU recommended city model based on LoS and NLoS rays segregation to simulate statistical parameters of the received power i.e. median and standard deviation in various urban environments.

4. **Models Evaluation and Comparison:** We perform analysis of the results obtained from the simulation results and the mathematical framework. In addition to this, numerical analysis of the SNR is performed for relay path in comparison with the direct path. Furthermore, we identify different parameters i.e. UAV location, and amplification factor to maximize the performance of an Amplify-and-Forward UAV based relay for providing enhanced coverage to the UEs. It is important to note that in this phase several iterations with previous two phases are conducted.

1.5 Thesis Organization

The remaining portion of this thesis is organized as follows:

- **Chapter 2 - Literature Review on 5G-UAV Relays Networks:** This chapter provides a consolidated summary of current research in 5G-UAV relay networks. The review focuses on UAV relay architectures, identifies the relevant gaps and challenges in deployment of 5G-UAV relay networks. It also sheds light on mmWave propagation characteristics and its path loss models.

- **Chapter 3 - Link-Level Performance Modelling 5G-UAV Relay Networks:** This chapter presents the technical contribution of this study to achieve objectives addressed by RQ1. We propose and describe the system architecture and link-level performance modelling of UAV use as an Amplify-and-Forward relay. We formulate mathematical framework for calculating UE received power for the direct path (between the gNB and UE) and the relay path (between the gNB and UE via UAV) based on two cases; (i) Friis Transmission Equation, and (ii) Log-Distance Path loss Model. For the proposed system architecture, we utilize ITU recommended city model to obtain the probability for LoS and NLoS paths in different urban environments. In addition to this, we study and analyze different parameters i.e., UAV location and amplification factor to maximize the performance of an Amplify-and-Forward UAV based relay for providing enhanced coverage to the UEs. This chapter concludes with the SNR analysis for the relay path compared with the direct path where we identify the constraints for effective relaying.

- **Chapter 4 - Simulations Results, and Discussions:** This chapter starts with illustrating simulations using ray-tracing simulator in different scenarios. We present comparison

and verification of the simulation results vs mathematical equations (which were derived in chapter 3) i.e., using both analytical approach and ray tracing simulator results. Furthermore, we evaluate, analyze and explain direct path and relay path using LoS and NLoS scenarios. Using ITU recommended city model and based on LoS and NLoS modes segregation, we simulate statistical parameters of received power i.e. median and standard deviation in various urban environments. This chapter concludes with the numerical analysis of SNR for the relay path in comparison with the direct path.

- **Chapter 5 - Conclusions and Future Work:** We conclude the thesis by summarizing major contributions of this study and possible future directions.

Chapter 2

Literature Review in 5G-UAV Relay

This chapter provides a consolidated summary of current research in 5G-UAV relay networks. The review focuses on UAV relay architectures, identifies the relevant gaps and challenges in the deployment of 5G-UAV relay networks. There is discussion on optimum placement of the UAVs as relaying and use of UAVs in mmWave band. It also sheds light on mmWave propagation characteristics and its path loss models.

2.1 UAV as Base Station Network Architectures

Use of UAV in cellular network is one of the key area of study, both in academia and industry in terms of its future attractiveness in wireless communication. In this section, a review of the most relevant related work on the network architectures involving UAVs are presented and summarised in Table 2.1.

In [24], the authors describe the opportunities and challenges of UAVs in wireless communication technologies. Firstly, an overview of UAV-aided wireless communications is presented as summarising the basic networking architecture for three practical scenarios: i) UAV-aided ubiquitous coverage under the overloaded base station (BS) or malfunctioning BS, ii) UAV-aided relaying, and iii) UAV-aided information dissemination and data collection. The paper also provides an overview of the UAV's main channel characteristics and design considerations taking into account both UAV-ground and UAV-UAV channels models. Finally, a key performance enhancing techniques that exploit the UAV's mobility is also discussed. Results are presented based on simulation under specific system parameter for path loss with static and mobile relaying. Results demonstrate that with mobile relaying, the UAV flies continuously between the source and destination aiming to reduce the link distances during both UAV information reception and

Table 2.1: Relevant summary on UAVs architecture for providing radio coverage.

Ref.	Research Direction/Main Idea	Evaluated KPIs	Main Conclusion	Challenges/Critical Analysis
Paper [24]	Channel characteristics and network architectures for three scenarios: i) UAV-aided ubiquitous coverage, ii) UAV-aided relaying, and iii) UAV-aided information dissemination and data collection	Path loss with static/mobile relaying	UAVs provides cost-effective wireless connectivity for devices without infrastructure coverage	Effective resource management and security mechanisms, constraints of UAVs and evaluation using mmWave frequency band.
Paper [23]	UAV-Mounted FSO Front-haul and Back-haul while using Edge Computing at RAN (EC-RANs)	End-to-end throughput	UAV mounted link is scalable and having low CAPEX/OPEX	Trajectory plan for UAV
Paper [25]	Bandwidth requirement for future UAVs as a function of UAV growth projections	Numbers of UAVs	Commercial UAVs will outnumber public agency UAVs especially small and micro UAVs	Careful infrastructure planning, replication of control elements, dedicated control links, UAVs route planning
Paper [26]	Resource allocation problem in UAVs networks with focus between reward and the power consumption	Optimal throughput of each small UAVs based based on payment ability and demand	Power and payment ability/demand	Coordination with the existing heterogeneous network. Evaluation of command center capabilities
Paper [27]	Effectiveness of UAV as relay in improvement of link reliability	Optimal path for UAVs	UAVs utility. Link availability and optimal paths can be planned for UAVs in order to maximize the network reliability	Path planning for solar-powered UAVs is required with energy constraints.
Paper [28]	RAN functionality splitting	Latency and data rate for split function options in C-RAN with the different front-haul media options	Convergence of front-haul and back-haul is beneficial	Precise and novel algorithm. Case study to assess QoS requirements.
Paper [29]	Functional split between centralized unit and distributed Unit	Data rate and latency	Higher splits and low data rate	Transport layer unification of current and new front-haul/back-haul traffic into a common-haul with SDN/NFV. Network planning and traffic management.
Paper [30]	mmWave BS incorporation with current cellular network	Coverage and data rate	Splitting user and data plan result in activating small cells (mmWave) only when needed. On demand data coverage	Coordinated centralised resource management and adaptive beam forming/beam tracking. Business continuity/service continuation evaluation. Optimal location for small (mmWave) cells in integration with HetNet.
Paper [31]	Spectrum pooling/sharing mechanisms using mmWave	Spectrum pooling performance	Spectrum pooling is advantageous	Cost efficiency evaluation and impact of real-world factors
Paper [32]	UAVs significance in multi-tier heterogeneous network	Coverage and capacity	UAVs deployment is productive	UAVs trajectory assessment
Paper [33]	Modeling Air-to-Ground path loss for low altitude platforms	Path loss	Path loss is dependent on elevation angle between between the terminal and the platform	Analysis with actual 3D-model and mmWave

relaying phases (data ferrying or load-carry-and-delivery). The authors conclude that: i) on-demand UAV systems are more cost-effective and can be much more swiftly deployed; suitable for unexpected or limited-duration missions, ii) short Range Light of Sing (LOS) potentially leads to significant performance improvement over direct communication between source and destination (if possible), and iii) manoeuvrability of UAVs offers new opportunities for performance enhancement. Finally , the authors point put that effective resource management and security mechanisms specifically designed for UAV communication systems are still needed. Additionally, high relative velocity between UAVs coupled with the higher frequency in the mmWave band could lead to excessive Doppler shift which is an area of study. *Even if the paper has a good cover of the challenges that UAVs communication faced, there is some missing points of this paper, for example, using the specific frequency bands of mmWave for UAV-UAV links to be used is not discussed.*

In [23], the authors discussed UAV-Mounted FSO Front-haul and back-haul while using Edge Computing at RAN (EC-RAN). At the beginning, a novel EC-RAN architecture is presented having two key considerations: i) where cache storage and light base band units (BBUs) are mounted on the UAVs to supplement the terrestrial infrastructure via UAV-mounted FSO-FnB links, ii) focus on the issues related to networking technologies and Communication Resource Management (CRM) in the EC-RAN with UAV-mounted FSO-FnB links. Outcomes were presented based on simulation which were performed under specific System parameter setting to show end-to-end throughput. Results suggest that throughput achieved by the UAV mounted FSO-FnB links outperforms that of the UAV-mounted RF-FnB links, and when the weather attenuation is larger than 57 dBm/km, the UAV is required to perform as a relay to compensate for the weather attenuation. The authors summarised that UAV mounted Front-haul and back-haul link using FSO with edge computing is scalable and having low CAPEX/OPEX. At the end, the authors underline some challenges i.e. requirements of practical algorithm for CRM to assist network dynamic metrics. *However, some areas which required further study and missed in the paper are i) using FSO in back-haul and access network while considering its limitations of physical obstructions, and ii) trajectory plan for UAV in terms Longitude, latitude and altitude for optimal service.*

In [25], the author describe bandwidth requirement for future Unmanned Aerial System (UAS) as a function of UAV growth projections. There is also an overview about new predictive models, and suitability of emerging spectrum sharing technologies for UAS. Initially, the authors highlighted that a UAS communications cell takes a 3D shape, such as a cone, sphere or cylinder, and may overlay with other cells. Moreover, different types of cells can be defined for different flight parameters (height, speed, etc.) and services (type of data and communications patterns) to ensure that critical communications services receive the highest protection. Mathematical equations were used to predict numbers of UAVs-in order to determine RF spectrum

requirements. Results indicate that commercial UAVs will outnumber public agency UAVs especially the small and micro UAVs (SUAV/MAV) which are low-altitude UAV alternatives:suitable for dense urban scenarios. The authors conclude that: i) UAV growth and RF spectrum are intertwined i.e. huge spectrum is required for growing number of UAVs, ii) an appropriate OFDM sub-carrier frequency spacing is suitable options to minimise inter-carrier interference (ICI) caused, among others, by the Doppler shift and carrier frequency offsets, iii)Spectrum allocations can be done on the basis of priorities, fairness, or more complex policies and rules. Finally, the authors emphasise the need for careful infrastructure planning, replication of control elements (databases, SASs), dedicated control links. *However, the missing point in the paper which required in depth study is algorithm for spectrum management with UAVs route planning.*

In [26], the author outline resource allocation problem in UAVs networks with focus between reward and the power consumption. Firstly, the authors presents a demand aware resource allocation mechanism for the information transmitting problem in UAV networks where a large UAV acts as a relay for small UAVs team. The relay UAV will act as cluster head, and is responsible mainly for: i) Resource allocation, and ii) centralised management. For results, stackelberg optimisation and Lagrange multiplier method have been used to find an optimal throughput of each small UAV under a given constraint power. Results indicate that system can transmit the total throughput decided by the upper hierarchy (Command Center), for allocating transmission rate to the lower hierarchy i.e. from relay UAVs to small UAVs) based on payment ability and demand. To Sum up, the authors conclude that: i) Command center assess the total performance of the system and has priority to make a decision firstly, and then the small UAVs team and the relay UAV according to the decision of the command center take actions, ii) Reward of each small UAV is influenced by the individual (UAV) demand and payment ability, iii) The stackelberg optimisation solution is feasible option for making a trade-off between information reward and the cost of total system. Furthermore, one-step glance back algorithm is shortlisted for finding the high level maximal utility convergence i.e. faster and precisely. *Nevertheless, the missing points in the paper, which need further study are: i) co-ordination of the current scenario with the existing heterogeneous Cellular network, and ii) evaluation of Command Center capabilities.*

In [27], the authors discussed back-haul links reliability problems in wireless balloon networks, and effectiveness of UAV as relay improvement of link reliability (or connectivity). In the beginning, the authors showed that using a few UAVs as relays can enhance connectivity among Wireless Balloon Networks by using an optimal paths that UAVs must follow to maximise the network reliability. Mathematical equations has been used to find out the optimal path for UAVs, which ll cover link outages. Simulations have been used for UAV utility vs. link availability by using three methods: i) optimal algorithm, ii) greedy algorithm, and iii) random selection. Results indicate that utility of UAV becomes less as the links become more available

i.e. an unreliable network could better utilise a UAV. Lastly, the main conclusions in the paper are: i) UAVs are used as relays to improve the reliability of wireless back-haul networks consisting of balloons, ii) given the link availability prediction, optimal paths can be planned for UAVs in order to maximise the network reliability (connectivity).Further area for research highlighted in the paper is path planning for solar-powered UAVs while keeping in consideration energy constraints. *However, analysis of Key Point Indicators (KPIs) for Customer Quality Experience (CQE) need further research too which is missing in the paper.*

In [28], the author describe different functional split options in C-RAN, available front-haul technologies, and the convergence of front-haul and back-haul technologies. Firstly, the authors propose a novel concept to split the RAN functionality into two parts i) One executed locally at the BS, ii) One executed at a central processing unit. As per authors, there are many factors that determine the required data rate for each split, and there are numerous options to split the RAN processing. However, only four major and representative options that show how the required FH capacity scales with the chosen functional split has been discussed. For results, existing available data (from the industry), latency and data rate were evaluated for the four split function options in C-RAN with the different front-haul media options. Key outcome is that convergence of FH and BH becomes necessary to avoid the need to deploy two separate transport networks. Conclusions deduced from split options in C-RAN are: i) for Layer-1, optimal media options are fibre, mmWave, and FSO respectively, ii) for layer-2, unified data plane need to design despite the diversity of exchanged information, iii) for Layer-3, future packet switches may need to support a more deterministic model, that is, guarantees on upper bounds for latency, jitter and packet loss rate, iv) Control and management planes need to enable joint optimisation of traffic steering in the transport network and RAN function placement across cloud nodes (i.e. using SDN, Network Functions Virtualisation). Finally, as per author, by adapting the functional split to the availability of the converged FH/BH network as well as actual user requirements, multiplexing gains can be exploited that further reduce the overall requirements. *However, there is a need for precise and novel algorithm to be used/studied for supporting converged FH/BH network while using split functions.*

In [29], the authors gives an overview on front-haul and back-haul wireless transport over mmWave for 5G with discussion on data rate and latency for front-haul interfaces. In the beginning, functional split between CU (Centralised Unit) and DU (Distributed Unit) in C-RAN is proposed in three splits: i) PHY-RF split, ii) Intra-PHY split, and iii) PDCP-RLC split. The authors make comparison for data rate and latency requirements for each of the above split options, based on some assumptions, such as number of antennas, number of ports. Results demonstrate that higher functional splits required low data rate and reasonably high latency ,and vice-versa. Moreover, the authors conclude that mmWave-based wireless back-haul/front-haul solutions are good alternatives in contrast to optical fibre with two possible situations: i)

Capped at the frequency 100 GHz including V and E bands where prototypes/commercial-grade products have appeared, ii) Bands above 100 GHz (W and D) are less intense despite their great potentials and needs further exploration for real deployment. At the end, the authors pin down the need for in depth study and analysis of using W-Band and D-Band which offer total channel bandwidth of 17.85 GHz and 31.8 GHz respectively. *Nonetheless, the missing point in the paper is to analyse the area of unifying the transport network of existing and new front-haul/back-haul traffic into a common-haul SDN/NFV (Software-defined networks and network function virtualisation) based packet switching network.*

In [30], the author discussed the use of mmWave in back-haul and access link in the current cellular network. At the beginning, the author propose a concept of a mmWave overlay in heavily populated heterogeneous networks (HetNet), where small cell base stations using mmWave are incorporated into traditional cellular networks, and there is logical split between control and user plane. A logical Network Access Entity (NAE) which can be implemented as a network virtual function for facilitating; resource assignment with a larger view on several parameters, at both user and network side. Based on wireless communication concepts and referencing from research papers authors figure out that, logical splitting control and user plane for UE will results in full coverage for very high data rates in the coverage area of mm-wave small cells. The authors main conclusions are:

- Splitting user and data plan will result in activating small cells only when needed, on demand data coverage, which means energy saving too,
- License free 60 GHz band having 9 GHz of unbroken spectrum having high propagation loss in free space due to oxygen absorption which comforts interference between neighbourhood connections,
- RMS delay spread of mmWave outdoor channels are almost same order for indoor and in-cabin propagation.

At the end, the authors highlight the necessity for further study on coordinated centralised resource management and adaptive beam forming /beam tracking. *However, primary area missing in the paper was to evaluate business continuity (i.e. service continuation) in case of outage in Small (mmWave) cells.*

In [31], the authors describe spectrum sharing between multiple operators, also referred to as spectrum pooling while taking considerations of mmWave. Firstly, authors gives an overview on different pooling mechanisms which are: i) interface at the RAN (BS), ii) interface at the CN, iii) RAN sharing, iv) CN sharing, v) via a spectrum broker, and vi) Uncoordinated. For results, predefined parameters i.e. number of operators, BS, UEs, bandwidth and frequency were considered using mmWave. Outcome indicates that under ideal assumptions, spectrum pooling is advantageous, and it delivers better performance to the 5th, 50th, and 95th percentile

users. Moreover, the authors conclude that mmWave communications have recently emerged as a solution to the spectrum scarcity in bands traditionally used for cellular communications and spectrum pooling at mmWave could allow more efficient use, and coordination among the networks of different operator can enhance spectrum pooling. Finally, the author underpin the need for further work to better understand impact of real-world factors, including; imperfect CSI, realistic antennas, back-haul latency, BS synchronisation, and distributed coordination. *Nevertheless, the cost efficiency in terms of OPEX, and CAPEX is an area of further study and exploration (in this scenario) which is missing in the paper.*

In [32], the authors discussed significance of drones in multi-tier heterogeneous network for improvement of network capacity, and coverage. Firstly, the authors investigated downlink (DL) transmission scheme having a high-power BS and UAVs (operating in the microwave band), alongside low-power small BSs (SBSs) operating in mmWave frequency band. Based on the user associations, the users can be classified into three different type: i) microwave BS and the SBSs operating at 28 GHz attempting to capitalise attainable energy efficiency of their associated users, ii) 73 GHz SBSs attempting to capitalise the attainable data rate of their associated users, and iii) UAVs functioning at the minimum power level to upkeep the minimum QoS requirements of their associated users. Results indicates that i) Optimal altitude of a UAV is directly proportional to cosθ where θ is the UAV's beam width angle, and inversely proportional to the cumulative additional losses (for both LOS and NLOS communication links), ii) achievable system Energy Efficiency (EE) is approx. two times more than the witnessed performance in the cellular networks without UAVs for all three considered power allocation methods. Furthermore, the authors concluded that UAV deployment is suitable for achieving high data rates, while sustaining the power consumed by the wireless infrastructure at a tolerable level. However, trajectory of UAV has not been considered in investigation, and the same observations needed to be evaluated while using mmWave at UAVs BS.

In [33], the authors discussed importance of airborne wireless BSs in cellular network, prediction of Path loss for air-ground channel (at low altitude), and its dependency on primary factor. At the beginning, the authors proposed statistical propagation model for foreseeing the air-to-ground path loss between a Low Altitude Platform (LAP) and a terrestrial User Element. Outcomes were presented based on mathematical equation and simulations in Wireless in suite for three different frequencies (700 MHz, 2000 MHz and 5800 MHz), and four virtual-cities (generated using a script writing in MATLAB) with reference to International Telecommunication Union (ITU-R) document recommendations, and taking into consideration of reflection, scattering, and diffraction. The authors summarised that in an urban environment, path loss for Air-Ground Channel (at low altitude) is dependent on elevation angle between the terminal and the Serving BS. *However, same observations need to be evaluated while extracting the actual 3D-model rather than readily available urban parameters, and QoS parameters conformance as*

well for terrestrial terminals.

2.1.1 Gaps and Open Challenges

As discussed in the literature review, there are still many open challenges of using UAV-relays for radio communications may face. In the following, the main gaps identified from the literature review are listed as follow:

- Finding suitable transmission medium for the Back-haul and Access communication links (simultaneously). Network planning and traffic management in this scenario is another thought-provoking area.
- The development of effective interference mitigating techniques specifically designed for the UAV-aided cellular coverage.
- Appropriate evaluation mechanisms are required to assess QoS requirements from user/application perspective and identifying relevant Key Performance Indicators (KPI).
- Achieving Transmitter(Tx)/Receiver(Rx) beam alignment for directional mmWave communications is a challenge to cover as well.
- Another main challenge stems from the size, weight, and power (SWAP) constraints of UAVs, which could limit their communication, computation and endurance capabilities.
- Energy-aware deployment and energy-efficient operation of the UAVs for mobility and communications needs to be address.
- Optimal location (co-ordinates) for small (mmWave) cells in integration with HetNet network require an in-depth study.

2.2 Relay in Cellular Communication

Relaying is a promising aspect of future wireless networks. 3GPP Release 10/11 (LTE-A) and IEEE 802.16j visualised the application cases scenarios, illustrated in Fig. 2.1:

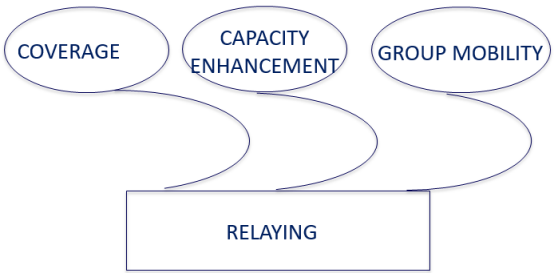

Figure 2.1: Relaying in cellular networks.

- **Capacity Enhancement:** UAVs have a immense potential to augment capacity of cellular networks i.e. to increase data rate, densifying an existing network and to cope with high traffic demands especially in dense urban areas or special events. Besides the long-range connectivity, multiple UAVs anchorage can facilitate better load balancing and traffic offload [34].
- **Group Mobility:** The mobility models are application dependent e.g. aggregating traffic of group users within a high-speed train or bus. Group mobility in mobile networks can cause degradation in network quality because of dynamic changes of network utilization [35]. Efficient placement of UAVs can reduce the strain on existing network in such scenarios and provide quality network acquisition.
- **Coverage:** To provide UE's signals of acceptable network, especially in shadowed zones. Cellular connectivity for UAV systems is interesting because it promises coverage in beyond visual line of sight scenarios [36]. In our work, providing coverage through UAVs is the main focus.

Different cooperative diversity protocols can be employed in this context. UAVs integration as relay into next generation wireless network needs efficient UAVs placement to enhance overall system efficiency. Broadly, cooperative diversity protocols can be classified into three categories based on the type of processing and requirements by relay and destination terminals, highlighted in Fig 2.2 [37].

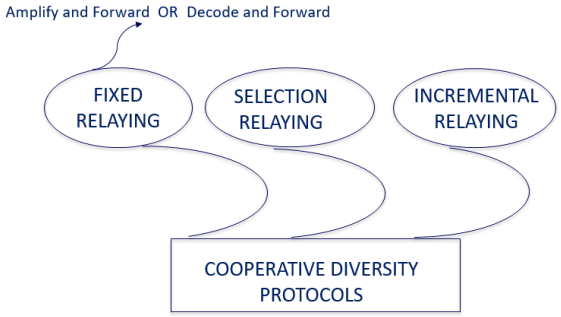

Figure 2.2: Cooperative diversity protocols

- **Fixed Relaying:** Relay works as Amplify-and-Forward (amplify the received signal subject to their power constraint) or decode and forward relay, and then re-transmit the signal.
- **Selection Relaying:** Adaptive strategies are followed. Relay selects a suitable cooperative/non-cooperative action based on SNR between the transmitting terminal and the relay.
- **Incremental Relaying:** It enhances spectral efficiency of both selection and fixed relaying by getting limited feedback form the destination terminal, and relaying when required.

2.2.1 Radio Relay Technologies

UAV-gNB can be used as a relay in various scenarios depending on the relay technology adopted. Broadly, it can be classified in three categories as illustrated in Fig. 2.3 [1].

- **Layer 1 Relay**: In this case, the received signal from Tx will be relayed (amplified and forwarded) to the respective Rx. This is called repeater or booster or more specifically an Amplify-and-Forward relay. One major disadvantage of such relay is that noise will also be amplified with the desired signal. However, the simplicity and inexpensiveness of this relay far outweigh the benefits.
- **Layer 2 Relay**: In this case, the received signal from Tx will be amplified and forwarded to the respective Rx and additional functions like modulation, demodulation, coding and decoding are performed as well. These functions facilitate in elimination of the noise.
- **Layer 3 Relay**: In this type of relay technology, the layer 3 functions such as user data regeneration processing are performed as well as layer 2 functions plus amplification of the received signal. Layer 3 relay also allows eradication of the noise but at the cost of increased processing delay.

Moreover, Table 2.2 highlights the benefits and drawbacks of all the three radio relay technologies.

Table 2.2: Comparison of radio relay technologies [1].

Relay Technology	**Advantages**	**Disadvantages**
Layer 1 Relay (Amplify-and-Forward Relay)	• Simple functionality • Inexpensive, easy to integrate with an existing network	• Amplification of the noise with the desired signal
Layer 2 Relay (Decode-and-Forward Relay)	• Noise Elimination • Layer 2 functions configuration facility i.e, modulation, demodulation, coding and decoding	• Increased processing delay due to layer 2 functions. • Addition of radio control functions between base station and relay station
Layer 3 Relay	• Noise Elimination • Layer 3 and layer 2 functions configuration facility i.e, user data regeneration processing, modulation, demodulation, coding and decoding	• Expensive, complex functionality and configuration • Increased processing delay due to layer 3 and layer 2 functions. • More prone to interference

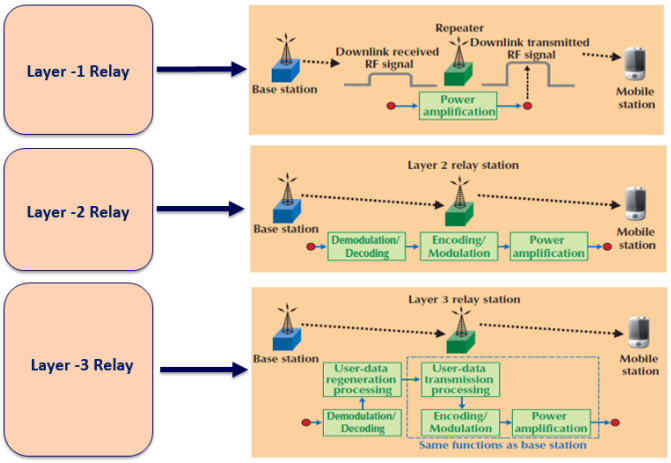

Figure 2.3: Relay in Cellular Communication [1]

2.3 Optimum Placement of UAVs as Relaying

Different researchers have studied, explored and analysed optimum placement of UAVs as UAV-aided base station. In [38], the authors explained UAV-BS optimum placement in device-to-device communication scenarios. The authors derived a controllable framework was for analysing coverage and data rate by evaluating different scenarios with the help of simulator measurements and analytical results. At the end of paper, there is discussion about the coverage vs required time for UAV-BS to cover the desired area (delay), in terms of stop points. In [33], path loss models were suggested for LoS and NLoS conditions. The authors discussed importance of airborne wireless BSs in cellular network, prediction of path loss for Air-Ground Channel (at low altitude), and its dependency on primary factor (elevation angle). At the beginning, the authors proposed statistical propagation model for foreseeing the air-to-ground path loss between a Low Altitude Platform (LAP) and a terrestrial UE. Outcomes were presented based on mathematical equation and simulations in Wireless InSite for three different frequencies (700 MHz, 2000 MHz and 5800 MHz), and four virtual-cities (generated using a script writing in MATLAB) with reference to ITU-R document recommendations and taking into consideration of reflection, scattering, and diffraction. The authors summarised that in an urban environment, path loss for air-ground channel (at low altitude) is dependent on elevation angle between the terminal and the serving BS.

In [19], effectiveness of UAV aid BS in cellular communication was studied and optimal placement of UAV-BS was conducted in consideration to 3D space. Simulations were performed for evaluating the performance in different scenarios. Main focus of this study was exploring the trade-off between maximising the number of users while keeping minimum transmit power. In [39], coverage probability of UAV-BS especially for downlink link was studied and analysed in relation to antenna gain and UAV-BS altitude. Circle packing theory was used, and coordinates

of UAV-BSs were determined in a way to increase coverage area and UAV-BS life time. The authors also highlighted the UAV altitude adjustment for mitigating interference. At the end of paper, there is discussion about the minimum number of UAVs required for providing coverage for a given terrestrial area. In [40], impact of UAV-BS height over an area, where UAV-BS is providing coverage to the users was explored. The authors investigated the availability of optimum UAV-BS height (in case of Rician fading), where coverage area can be maximised. At the end of the paper, formulas for the optimal height and maximum coverage radius were provided.

In [34], author studied the optimal placement and distribution of UAV-BS in future wireless cellular networks with focus on minimising network delays. The authors proposed a strategy of UAV-BSs allocation to the demand area using idea of entropy nets. At the end, the author highlighted the optimisation of network delays while having no impact on capacity and coverage. In [24], the authors describe the opportunities and challenges of UAVs in wireless communication technologies. Firstly, an overview of UAV-aided wireless communications is presented as summarizing the basic networking architecture for three practical scenarios: i) UAV-aided ubiquitous coverage under the overloaded base station (BS) or malfunctioning BS, ii) UAV-aided relaying, and iii) UAV-aided information dissemination and data collection. Results are presented based on simulation under specific system parameter for path loss with static and mobile relaying. In [41], authors examined connectivity and coverage of UAV-BS with focus on observing an area of interest by suggesting connectivity-based mobility model between UEs and UAV-BS. Different scenarios were explored to show the trade-off between quality network acquisitions by UAV-BS and remain connected with UEs. In [42], main focus of study was backhaul link between UAV-BS and terrestrial BS. User-centric and Network-centric methodologies were proposed and optimal 3D backhaul-aware placement of a drone-BS is explored. The authors also focused on UAV-BS battery vs channel variations and UAV-BS flight time. However, key areas which required in depth study and analysis are:

- SWAP constraints of the UAVs.
- Link performance of UAV relay using mmWave at the Backhaul and Access link.
- Analysis/optimisation of different optimal parameter to maximise the performance.
- Optimal trajectory for the UAV.

2.4 5G Spectrum Frequency Bands

5th Generation cellular technology represents a massive leap forward for wireless mobile communications, far surpassing 4G (LTE/Advanced/Advanced Pro, WiMax), 3G (UMTS/WCDMA, CDMA/1xEV-DO), and 2G (GSM/GPRS, CDMA/1xRTT) communication platforms in terms

of data rate and reduced latency. In order to support all the requirements it promises to deliver, massive quantities of new radio spectrum (5G NR frequency bands) have been allocated to 5G, notably in millimeter-wave bands [2; 43]. The basic idea for 5G is to use frequency spectrum above 6 GHz which will provide enough bandwidth to every user that higher data rates are possible [44]. 5G technology can employ cm-waves to mm-waves frequencies ranging from 20 GHz to up to 300 GHz. 3GPP Release-16 is expected to be standardized by 2020 [7], however, 3GPP Release 15-the first full set of 5G standards is released in 2019 [6]. In our analysis and observation, we consider 28 GHz frequency band which is the part of the 5G frequency RF plan [45; 46]. Fig. 2.4 depicts the 5G spectrum frequency bands. For addressing the diversi-

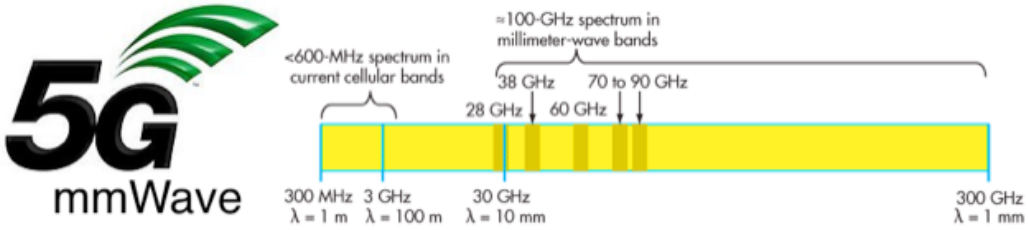

Figure 2.4: 5G spectrum frequency bands.

fied requirements from the envisioned 5G usage scenarios, 5G needs access to "low", "medium" and "high" frequencies, illustrated in Fig. 2.5. A sufficient amount of harmonised spectrum in each layer should be made available by national regulators in a timely manner to enable mobile operators to deliver 5G services.

Figure 2.5: Multi-layer frequencies approach for 5G usage scenarios [2].

2.5 UAVs in mmWave Band

Wider bandwidth availability in mmWave has attracted both the academia and researchers attention for its use in next generation wireless networks. Reduced antenna size at the tiny wavelength band has made it even more suitable in terms of lighter weight as payload in aerial communications [47]. In addition to this, multi-stream, multi-beam and multi-user (MU) communications features is another positive aspect of utilising mmWave band. Until the present time, there is limited work on mmWave air-to-air and air-to-ground channel modelling. Although, aerial communication is different from terrestrial channel models because they have lower path loss exponent and smaller small scale fading [48]. However, mmWave links constraints UAV-gNB from using high altitude due to its intrinsically high path loss with regards to the growing distance from transmitter to receiver, so terrestrial channel models can be applied to mmWave aerial communication scenarios as well; where UAV-gNB will be placed at the same height as of the terrestrial base station [49; 50; 51]. Nonetheless, while using mmWave, antenna patterns, blockage environment and fading channel model must be cautiously adapted. In [52], author presented a 3D sectored pencil beam pattern for mmWave antenna. Likewise, Nakagami-m fading channel was considered more suitable in mmWave communication links due to enormous difference between NLoS and LoS signal strengths [52; 53; 54; 55]. In [56], author described 3D analytical framework by introducing a 3D sectorized antenna and 3D blockage model while simultaneously considering UAVs and UEs altitude. In [57], authors proposed a methodology for optimal height, coverage radius and coordinates of UAV configured as base stations while considering blockage by human body. Furthermore, for integrating UAV configured as base station into heterogeneous next generation wireless networks, concept of network slicing was introduced i.e. providing a network slice for necessary backhaul, front-haul, and network functions while considering the mobility of UAV-BS [49]. UAVs integration into next generation wireless network needs efficient UAVs placement to enhance overall system efficiency.

Nevertheless, the primary areas requiring in-depth study and analysis are as follows:

- Evaluating the link performance of UAV-gNB relay using mmWave at the backhaul and Access link.
- Analysis/optimisation of key parameters to optimize the performance.
- Integration of the UAV-gNB using mmWave in Backhaul and Access link with the existing heterogeneous networks i.e. 3G, LTE, and 5G.
- The practical implementations of designing practical antenna array on chip while using mmWave.

2.5.1 Path Loss Models for mmWave Band

Several path-loss models has been proposed in literature based on extensive measurements performed in 73 GHz, 60 GHz, 38 GHz, and 28 GHz frequency bands, summarised in Table 2.3. However, we are using Log-distance path loss model in our analysis and observation.

Table 2.3: Relevant mmWave path loss models.

Path Loss Model	**Summary**	**Measurement Frequency**	**Project**	**Critical Analysis**
Reference Path Loss Model (RPLM) or Log-Distance Path loss model [58; 59; 60; 61; 62; 63; 64; 65]	Calculating path loss at reference distance d_0, having dependency on only one variable n_p	28 GHz, 38 GHz and 60 GHz,	MiWEBA, IEEE 802.15.3c, and NYU projects,	Having dependency on single parameter.
Modified Path Loss Model (MPLM) [65; 66; 67; 68]	Considered as an updated version of RPLM	28 GHz and 73 GHz,	WINNER II and 3GPP projects,	Two parameters facilitate higher degree of freedom in calculation and analysis.
Dual Slope Path Loss Model (DSPLM) [59; 65; 69]	Extension of MPLM, where extrapolation operations was considered i.e. including path loss values at 400 m rather than 200 m,	28 GHz,	NYU project	More suitable for calculating path loss of values at greater distances than 200 m up-to 400 m.

2.5.1.1 Log-Distance Path Loss Model

Path loss between the Tx and Rx over a distance d (m) at a given carrier frequency f (Hz) is given by [58; 59; 60; 61]:

$$\mathrm{PL(d)} = \mathrm{PL(d_o)} + 10\ \alpha\ log_{10}(\frac{d}{d_o}) + N(0, \sigma^2) \tag{2.1}$$

where:

- PL(d) is the path loss in dB at distance d,
- d_o is the reference distance equal to 1 m,
- $\mathrm{PL(d_o)} = 20\ log_{10}(\frac{4\pi d_o}{\lambda})$ is the path loss at the reference distance,
- α is single path Loss exponent (PLE), which describes the attenuation of signal as it propagates in the channel. It is obtained through best fit (MMSE) over all measurement for a particular measurement campaign,

- $N(0, \sigma^2)$ is the Zero mean Gaussian random variable (shadowing),
- d is the distance between the Tx and the Rx where $d \geq d_o$,

This model is used for MiWEBA and IEEE 802.15.3c projects [62; 63]. This model use a single parameter α, and referencing d_o equal to 1 m. Normally, 1st meter of propagation has no obstruction from transmiter antenna which enhance the effectiveness of this model as standard path loss modelling methodology for mmWave band. Moreover, Table 2.4 summarize the Path loss exponent and standard deviation values of Log-Distance Path loss Model determined in measurement campaign [3; 4].

Table 2.4: Path loss exponent and standard deviation values for Log-Distance Path loss Model obtain in the measurement campaign [3; 4].

Scenario	**Environment**	**Frequency [GHz]**	**Path Loss Exponent**	**Standard Deviation [dB]**
Urban Macro	LoS	2	2.0	1.7
Urban Macro	NLoS	2	2.8	3.5
Urban Macro	LoS	10	2.0	3.1
Urban Macro	NLoS	10	3.1	4.1
Urban Macro	LoS	18	2.0	2.0
Urban Macro	NLoS	18	3.0	4.5
Urban Macro	LoS	28	2.0	2.3
Urban Macro	NLoS	28	2.7	4.9
Urban Macro	LoS	38	1.9	3.5
Urban Macro	NLoS	38	2.7	10.5

Chapter 3

Link-Level Performance Modelling 5G-UAV Relay

This chapter presents the technical contribution of this study to achieve objectives addressed by RQ1. We propose and describe the system architecture and link-level performance modelling of UAV-gNB use as an Amplify-and-Forward relay. We formulate mathematical framework for calculating UE received power for the direct path (between the gNB and UE) and the relay path (between the gNB and UE via UAV) based on two cases; (i) Friis Transmission Equation, and (ii) Log-Distance Path loss Model. For the proposed system architecture, we utilize ITU recommended city model to obtain the probability for LoS and NLoS paths in different urban environments. In addition to this, we study and analyze different parameters i.e., UAV location and amplification factor to maximize the performance of an Amplify-and-Forward UAV based relay for providing enhanced coverage to the UEs. This chapter concludes with the SNR analysis for the relay path compared with the direct path where we identify the constraints for effective relaying.

3.1 System Architecture Description

The proposed system architecture of this study is depicted in Fig. 3.1, showing an aerial-terrestrial network based on the combination of traditional terrestrial base station (gNB) communicating with UAV equipped with an Amplify-and-Forward relay (UAV). The Back-haul link between the gNB and the UAV is using mmWave link as well as the Access link (UAV-UE) is providing coverage to the UEs through mmWave.

Motivated by the adoption of terrestrial channel models for air-to-ground channels of static UAV-gNB, UAV is deployed as a quasi-stationary aerial gNB behaving like an orthodox cell tower [49; 50; 51] (hence Doppler effect is not considered in this study). High data rate mmWave

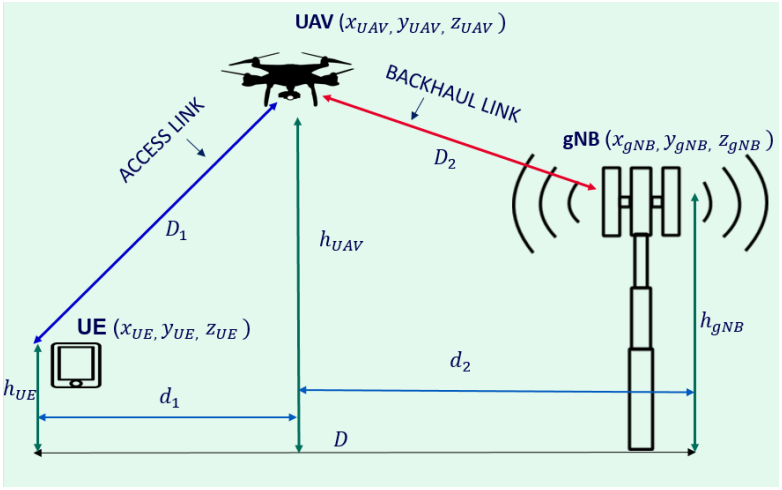

Figure 3.1: The proposed system architecture for UAV relay using mmWave.

links constraints UAVs from using high altitude due to its intrinsically high path loss with growing distance from Tx to Rx. Consequently, the altitude of a UAV must be carefully planned. Additionally, the intrinsic high path loss feature of mmWave necessitates the optimal deployment of mmWave UAV in consideration to three dimensional (3D) placement analysis from Tx to Rx. Isotropic antennas are considered for simplifying the analysis. Arbitrary antenna patterns and Multi Input Multi Output (MIMO) can be easily adoptable with the available isotropic model. Unlike the terrestrial gNB, UAV can provide dynamic coverage and has become mature in terms of light weight and longer battery life [70]. In this study, the UAV is deployed as a layer 1 Amplify-and-Forward relay which can be readily incorporate in a cellular communication system. System parameters and notations are described in Table 3.1.

In Amplify-and-Forward relay technology, radio frequency signals received on downlink from gNB and uplink from UE are amplified by an amplification factor (β) and transmitted, respectively [1]. Importance of an amplification factor is to mitigate the path loss. Because, the amplification process is performed in the physical layer domain, the noise is amplified inadvertently, which limits the overall efficiency of the system. It is a trade-off between performance and complexity at the relay terminal, where simple function, low implementation cost and short processing delay in Amplify-and-Forward relay technology has resulted in its widespread usage in the cellular networks.

3.2 Link-Level Performance Modelling

At mmWave frequency band, accurate channel modelling is an important prerequisite to design an efficient wireless communication network; especially for fostering new techniques that can comply with its propagation characteristics. Broadly, channel models can be divided into two sub-categories: analytical and physical models [71].

Table 3.1: Notation and parameters used for modelling.

Description	Parameter	Unit
Unmanned Aerial Vehicle relay	UAV	-
User Equipment	UE	-
gNB coordinates	$(x_{\text{gNB}}, y_{\text{gNB}}, z_{\text{gNB}})$	-
UAV coordinates	$(x_{\text{UAV}}, y_{\text{UAV}}, z_{\text{UAV}})$	-
UE coordinates	$(x_{\text{UE}}, y_{UE}, z_{\text{UE}})$	-
gNB height	h_{gNB}	m
UAV height	h_{UAV}	m
UE height	h_{UE}	m
Distance between gNB and UAV	D_2	m
Distance between UAV and UE	D_1	m
Horizontal distance between gNB and UAV	d_2	m
Horizontal distance between UAV and UE	d_1	m
Horizontal distance between gNB and UE	D	m
UE received power via the direct path	$P_{\text{UE-D}}$	dBm
UE received power via the relay path	$P_{\text{UE-R}}$	dBm
UAV received power	$P_{\text{UAV-r}}$	dBm
gNB transmitted power	P_{gNB}	dBm
UAV transmitted power	$P_{\text{UAV-t}}$	dBm
gNB antenna gain	G_{gNB}	dBi
UAV antenna gain	G_{UAV}	dBi
UE antenna gain	G_{UE}	dBi
UAV antenna gain	G_{UAV}	dBi
Amplification factor of the UAV	β	dB
Path Loss Exponent (PLE): gNB–UE link	α	-
Path Loss Exponent (PLE): UAV–UE link	α_1	-
Path Loss Exponent (PLE): gNB–UAV link	α_2	-
Zero mean Gaussian random variable: gNB–UE link(shadowing)	$N(0, \sigma^2)$	
Zero mean Gaussian random variable: UAV–UE link(shadowing)	$N(0, \sigma_1^2)$	-
Zero mean Gaussian random variable: gNB–UAV link(shadowing)	$N(0, \sigma_2^2)$	-
Standard deviation for gNB-UE	σ	
Standard deviation for UAV-UE	σ_1	-
Standard deviation for gNB-UAV	σ_2	-

- Analytical models: mathematical analysis of channel,
- Physical models: exploring the electromagnetic properties of the signal from Tx to Rx [72].

Analytical models are either propagation based or correlation-based, while physical models are either deterministic or stochastic, illustrated in Fig. 3.2. We considered propagation based Friis Transmission Equation and Log-Distance Path Loss model for the analysis and observations.

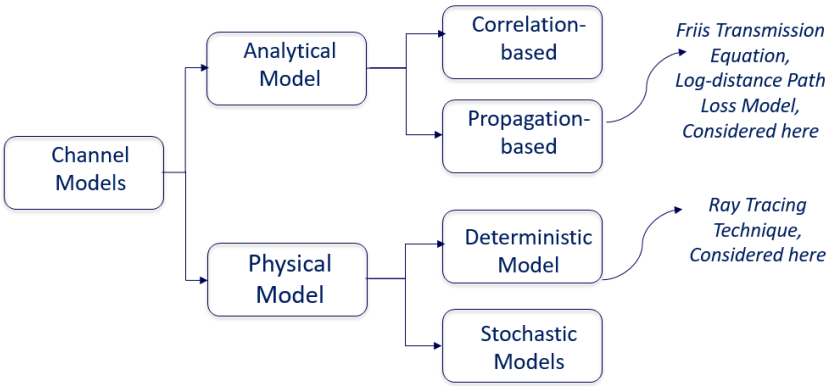

Figure 3.2: Channel models techniques explored in this study.

3.2.1 Direct Path: gNB-UE (Based on Friis Transmission Equation)

Mathematical modelling has received significant importance in understanding wireless signal propagation characteristics. It provides a recipe on how to simplify an observed phenomenon and to obtain a computationally tractable description. Using Friis Transmission Equation and referring to Fig. 3.3, the received power by UE via direct path is given by [73]:

$$P_{\mathrm{UE-D}} = P_{\mathrm{gNB}} + G_{\mathrm{UE}} + G_{\mathrm{gNB}} - 20\ log_{10}\left(\frac{\lambda}{4\pi D}\right) \tag{3.1}$$

where,

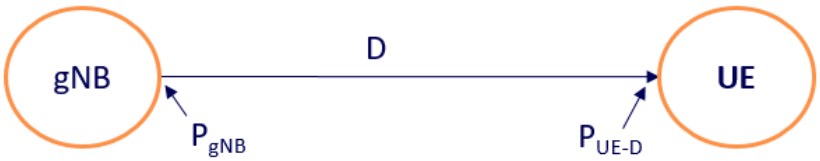

Figure 3.3: Base station to user equipment communication.

- $P_{\mathrm{UE-D}}$ is the UE received power in dBm,
- P_{gNB} is the gNB transmitted power in dBm,
- G_{gNB} is the gNB antenna gain,
- G_{UE} is the UE antenna gain,
- λ is wavelength of the signal from the gNB to the UE in m,
- D is the Euclidean distance between gNB and UE, is given by:

$$D = \sqrt{(x_{\mathrm{UE}} - x_{\mathrm{gNB}})^2 + (y_{\mathrm{UE}} - y_{\mathrm{gNB}})^2 + (z_{\mathrm{UE}} - z_{\mathrm{gNB}})^2} \tag{3.2}$$

3.2.2 Direct Path: gNB-UE (Based on mmWave Log-Distance Path Loss Model)

Using Log-Distance path loss model, which is based on single parameter α that represents the path loss exponent and referring to Fig. 3.3, the path loss from gNB to UE is given by [58; 59; 60; 61; 62; 63; 64; 65; 71]:

$$\mathrm{PL(D)} = \mathrm{PL(d_o)} + 10\ \alpha\ log_{10}\left(\frac{D}{d_o}\right) + N(0, \sigma^2)$$

where,

- PL(D) is path loss from gNB to UE in dB,
- d_o is equal to 1m as reference distance,
- $\mathrm{PL(d_o)} = 20\ log_{10}(\frac{4\pi d_o}{\lambda})$ is the path loss at the reference distance,
- α is the Path Loss Exponent (PLE) for gNB–UE link,
- $N(0, \sigma^2)$ is the Zero mean Gaussian random variable for gNB–UE link (shadowing),
- σ is the standard deviation.

The received power by UE via direct path can be expressed as:

$$P_{\mathrm{UE-D}} = P_{\mathrm{gNB}} - \mathrm{PL(D)} \tag{3.3}$$

3.2.3 Relay Path: gNB-UAV-UE (Based on Friis Transmission Equation)

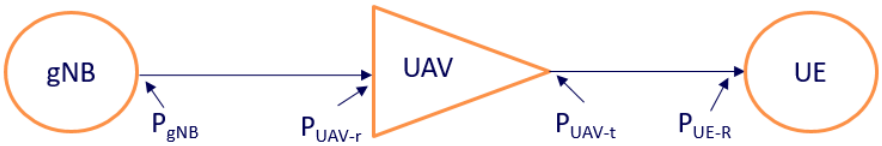

Figure 3.4: End-to-end representation of the gNB to the UE communication using a relay node.

Using Friis Transmission Equation and referring to Fig. 3.4, the received power by UE is given by [73]:

$$P_{\mathrm{UAV-r}} = P_{\mathrm{gNB}} + G_{\mathrm{UAV}} + G_{\mathrm{gNB}} - 20\ log\left(\frac{\lambda_2}{4\pi D_2}\right)$$

where,

- $P_{\mathrm{UAV-r}}$ is the UAV received power in dBm,
- P_{gNB} is the gNB transmitted power in dBm,

- G_{UAV} is the UAV antenna gain,
- G_{gNB} is the gNB antenna gain,
- λ_2 is wavelength of the signal from the gNB to the UAV in m,
- D_2 is the Euclidean distance between gNB and UAV, is given by:

$$D_2 = \sqrt{(x_{\mathrm{UAV}} - x_{\mathrm{gNB}})^2 + (y_{\mathrm{UAV}} - y_{\mathrm{gNB}})^2 + (z_{\mathrm{UAV}} - z_{\mathrm{gNB}})^2} \tag{3.4}$$

For simplifying the expressions, let:

$$k_2 = \left(\frac{\lambda_2}{4\pi}\right) = \left(\frac{c}{4\pi f_2}\right)$$

Thus, $P_{\mathrm{UAV-r}}$ can be written as:

$$P_{\mathrm{UAV-r}} = P_{\mathrm{gNB}} + \ G_{\mathrm{UAV}} + \ G_{\mathrm{gNB}} - 20 \ log_{10} \ \left(\frac{k_2}{D_2}\right) \tag{3.5}$$

When deploying UAV as an Amplify-and-Forward relay, the following amplification takes place as specified in [1]:

$$P_{\mathrm{UAV-t}} = \beta + P_{\mathrm{UAV-r}} \tag{3.6}$$

where,

- $P_{\mathrm{UAV-t}}$ is the UAV transmitted power in dBm,
- β is the amplification factor in dB,

By substituting in (3.5) and referring to Fig. 3.4, the received power by UE via relay path is given by:

$$P_{\mathrm{UE-R}} = P_{\mathrm{UAV-t}} + \ G_{\mathrm{UE}} + \ G_{\mathrm{UAV}} - 20 \ log_{10} \ \left(\frac{\lambda_1}{4\pi D_1}\right)$$

where:

- $P_{\mathrm{UE-R}}$ is the UE received power via UAV in dBm,
- λ_1 is wavelength of the signal from the UAV to the UE in m,
- D_1 is the Euclidean distance between gNB and UAV, is given by:

$$D_1 = \sqrt{(x_{\mathrm{UE}} - x_{\mathrm{UAV}})^2 + (y_{\mathrm{UE}} - y_{\mathrm{UAV}})^2 + (z_{\mathrm{UE}} - z_{\mathrm{UAV}})^2}$$

For simplifying the expressions, let:

$$k_1 = \left(\frac{\lambda_1}{4\pi}\right) = \left(\frac{c}{4\pi f_1}\right)$$

Thus, the received power by UE via UAV is:

$$P_{\mathrm{UE-R}} = P_{\mathrm{UAV-t}} + \ G_{\mathrm{UE}} + \ G_{\mathrm{UAV}} - 20\ log_{10}\ \left(\frac{k_1}{D_1}\right) \tag{3.7}$$

Substituting (3.5) and (3.6) in (3.7), assuming the same antenna gain for the Tx and Rx sides of the UAV, the received power of the UE via UAV is:

$$P_{\mathrm{UE-R}} = \beta + P_{\mathrm{gNB}} + \ G_{\mathrm{gNB}} + \ 2\ G_{\mathrm{UAV}} + G_{\mathrm{UE}} - 20\ log_{10}\ \left(\frac{k_2}{D_2}\right) - 20\ log_{10}\ \left(\frac{k_1}{D_1}\right) \tag{3.8}$$

In addition to the frequency and antenna gains, received bower by the UE has dependency on three main parameters:

- Distance between gNB and UAV (D_2),
- Distance between UAV and UE (D_1), and
- Amplification factor (β).

3.2.4 Relay Path: gNB-UAV-UE (Based on mmWave Log-Distance Path Loss Model)

Using log-distance path loss model and referring to Fig. 3.4, the path loss from gNB to the UAV is given by:

$$\mathrm{PL(D_2)} = \mathrm{PL(d_o)} + 10\ \alpha_2\ log_{10}\left(\frac{D_2}{d_o}\right) + N(0, \sigma_2^2)$$

where,

- $\mathrm{PL(D_2)}$ is path loss from gNB to UAV in dB,
- d_o is equal to 1m as reference distance,
- $\mathrm{PL(d_o)} = 20\ log_{10}(\frac{4\pi d_o}{\lambda})$ is the path loss at the reference distance,
- α_2 is the Path Loss Exponent (PLE) for gNB–UAV link,
- $N(0, \sigma_2^2)$ is the Zero mean Gaussian random variable for gNB–UAV link(shadowing),
- σ_2 is the standard deviation.

Path loss exponent and standard deviation values are listed in Table 2.4 for different frequencies obtained through measurement campaigns. The received power by the UAV can be expressed as:

$$P_{\mathrm{UAV-r}} = P_{\mathrm{gNB}} - \mathrm{PL(D_2)}$$

$$P_{\mathrm{UAV-r}} = P_{\mathrm{gNB}} - \mathrm{PL(d_o)} - 10\ \alpha_2\ log_{10}\left(\frac{D_2}{d_o}\right) - N(0,\sigma_2^2) \tag{3.9}$$

As per (3.6) and (3.9), the UAV transmitted power is given as:

$$P_{\mathrm{UAV-t}} = \beta + P_{\mathrm{gNB}} - \mathrm{PL(d_o)} - 10\ \alpha_2\ log_{10}\left(\frac{D_2}{d_o}\right) - N(0,\sigma_2^2) \tag{3.10}$$

Similarly, path loss from the UAV to the UE is given by:

$$\mathrm{PL(D_1)} = \mathrm{PL(d_o)} + 10\ \alpha_1\ \log_{10}\left(\frac{\mathrm{D_1}}{\mathrm{d_o}}\right) + N(0,\sigma_1^2) \tag{3.11}$$

where:

- $\mathrm{PL(D_1)}$ is the path loss from UAV to UE in dB,
- α_1 is the Path Loss Exponent (PLE) for gNB–UE link,
- $N(0,\sigma_1^2)$ is the Zero mean Gaussian random variable for gNB–UE link(shadowing),
- σ_1 is the standard deviation.

Similarly, the received power by UE via relay path is given by:

$$P_{\mathrm{UE-R}} = P_{\mathrm{UAV-t}} - \mathrm{PL(D_1)}$$

Substituting (3.8) and (3.9) in (3.10), received power by the UE is given by:

$$P_{\mathrm{UE-R}} = \beta + P_{\mathrm{gNB}} - 2\ \mathrm{PL(d_o)} - 10\ \alpha_2\ log_{10}\left(\frac{D_2}{d_o}\right) + 10\ \alpha_1\ log_{10}\left(\frac{D_1}{d_o}\right) - N(0,\sigma_1^2) - N(0,\sigma_2^2)$$

Substituting $\mathrm{PL(d_o)}$, received power by UE can be written as:

$$P_{\mathrm{UE-R}} = \beta + P_{\mathrm{gNB}} - 40\ log_{10}\left(\frac{4\pi d_o}{\lambda}\right) - 10\ \alpha_2\ log_{10}\left(\frac{D_2}{d_o}\right) + 10\ \alpha_1\ log_{10}\left(\frac{D_1}{d_o}\right) - N(0,\sigma_1^2) - N(0,\sigma_2^2) \tag{3.12}$$

3.2.5 LoS and NLoS Probabilities in Different Urban Environments

The knowledge of LoS and NLoS probability is crucial to estimate signal attenuation correctly in mobile wireless communication. Especially in built-up areas, more accurate LoS probability determination helps to obtain more realistic propagation models or path loss models. In this section, we utilize ITU recommended city model to obtain the probability for LoS and NLoS paths in different urban environments [74; 75]. Generally, there are three cases:

- **P(LoS)**: The Line of Sight probability corresponds to the probability that the signal from Tx to Rx will reach along an unobstructed propagation path (Zero reflection or scattering),

- **P(NLoS)**: The Non Line of Sight probability corresponds to the probability that the signal from Tx to Rx will reach along an obstructed propagation path (via one or more reflections or scattering),
- **Outage**: In this case, the path loss is sufficiently high or infinite i.e. having signal strength below the required threshold and can exist in both states.

Although, aerial communication is different from terrestrial channel models because they have lower path loss exponent and smaller small scale fading [48]. However, mmWave links constraints UAV-gNB from using high altitude due to its intrinsically high path loss with regards to the growing distance from transmitter to receiver, so terrestrial channel models can be applied to mmWave aerial communication scenarios as well; where UAV-gNB will be placed at the same height as of the terrestrial base station [49; 50; 51]. Probability of geometrical LoS between a terrestrial Tx at height h_{gNB} and Rx at height h_{UAV} (or h_{UE}) can be deduced from ITU recommended city model [5]. This probability has dependency on three statistical parameters:

- A is the ratio of built-up land area to the total land area (dimensionless).
- B is the mean number of buildings per unit area ($buildings/km^2$).
- C describes the building′s heights distribution according to Rayleigh Probability Density Function given by:

$$f(h_b) = \frac{h_b}{C^2} \ \exp \frac{-h_b^2}{2C^2}$$

  where, h_b is the building height in meters.

Assuming, evenly spaced building (on average) for the easy estimation of number of building between two points. The probability of LoS ray would be [5]:

$$\mathrm{P(LoS)} = \prod_{l=1}^{l_r} (P(h_b) < h_{\mathrm{gNB}}) \tag{3.13}$$

where,

- h_{gNB} is the height of the gNB
- l_r is the number of building crossed.

Following the ITU recommendation doc and related mathematical steps, the probability of LoS for gNB to UAV link can be written as [5; 33]:

$$\mathrm{P(LoS)}_{\mathrm{gNB-UAV}} = \prod_{p=0}^{q} \left[1 - \exp\Big(- \frac{\left[h_{\mathrm{gNB}} - \frac{(q+1/2)(h_{\mathrm{gNB}} - h_{\mathrm{UAV}})}{(q+1)} \right]^2}{2C^2} \Big) \right] \tag{3.14}$$

where,

- q=floor$(d_2\sqrt{AB}-1)$ and,
- d_2 is the ground distance between gNB and UAV,

Similarly, probability for LoS for UAV to UE link would be:

$$\mathrm{P(LoS)_{UAV-UE}} = \prod_{s=0}^{t}\left[1-\exp\Big(-\frac{\left[h_{\mathrm{UAV}}-\frac{(t+1/2)(h_{\mathrm{UAV}}-h_{\mathrm{UE}})}{(s+1)}\right]^2}{2C^2}\Big)\right] \tag{3.15}$$

where,

- $t = floor(d_1\sqrt{\alpha B}-1)$ and,
- d_1 is the ground distance between UAV and UE

Subsequently, probability of NLoS paths for gNB to UAV would be:

$$\mathrm{P(NLoS)_{gNB-UAV}} = 1-\mathrm{P(LoS)_{gNB-UAV}} \tag{3.16}$$

Similarly, probability of NLoS paths for UAV to UE link will be:

$$\mathrm{P(NLoS)_{UAV-UE}} = 1-\mathrm{P(LoS)_{UAV-UE}} \tag{3.17}$$

3.2.5.1 LoS and NLoS Probability Plotting

In order to plot the probability of LoS rays, we use the approach in [33]. Refer to Fig. 3.1, ground distance d_1 from gNB to UAV can be calculated as below:

$$d_1 = \frac{h_{\mathrm{UE}}}{tan(\theta)}$$

where: θ is UE elevation angle.

In literature [33], resulting plot for Eq. 3.17 becomes a continuous function of elevation angle and environmental parameters. Thus, the probability for LOS from UAV to UE is plotted in Fig. 3.6 for four urban environments described in Table 3.2.

Table 3.2: Urban environmental parameters [5].

Parameters	**Environment**	**Value**
$A,\ B,\ C$	Suburban	0.1, 750, 8
$A,\ B,\ C$	Urban	0.3, 500, 15
$A,\ B,\ C$	Dense Urban	0.5, 300, 20
$A,\ B,\ C$	High-rise urban	0.5, 300, 50

Referring to the Fig. 3.4, there are two links and four possible combination.

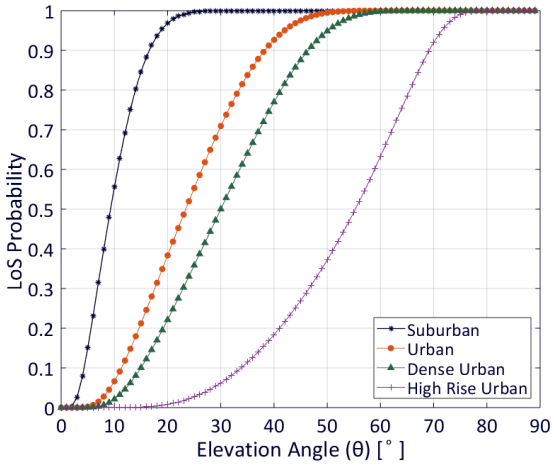

Figure 3.5: LoS probability for different urban environments.

$$\text{gNB } to \text{ UAV} = \begin{cases} \text{gNB } to \text{ UAV } (LoS) \\ \text{gNB } to \text{ UAV } (NLoS) \end{cases}$$

$$\text{UAV to UE} = \begin{cases} \text{UAV to UE } (LoS) \\ \text{UAV to UE } (NLoS) \end{cases}$$

Accordingly, the average path loss from gNB-UAV will be:

$$\overline{PL}_{\text{gNB}-\text{UAV}} = PL(LoS)_{\text{gNB}-\text{UAV}} \times P(LoS)_{\text{gNB}-\text{UAV}} + PL(NLoS)_{\text{gNB}-\text{UAV}} \times P(NLoS)_{\text{gNB}-\text{UAV}} \tag{3.18}$$

Likewise, the average path loss from UAV-UE will be:

$$\overline{PL}_{\text{UAV}-\text{UE}} = PL(LoS)_{\text{UAV}-\text{UE}} \times P(LoS)_{\text{UAV}-\text{UE}} + PL(NLoS)_{\text{UAV}-\text{UE}} \times P(NLoS)_{\text{UAV}-\text{UE}} \tag{3.19}$$

3.2.6 SNR Analysis

SNR is a wireless communication measure which is used to compare the level of the desired signal to the level of noise. SNR is defined as the ratio of signal power to the noise power expressed in decibels. A negative SNR indicates more noise than signal. SNR is a major component in the analysis and design of the link budget of a telecommunication system. In cooperative relaying, merit of using relay path need to be assessed based on the SNR of the received signal. In our analysis, we are using an Amplify-and-Forward relay, to bring the signal strength to a certain level by the amplification factor (β). However, noise is always present with the input signal and amplifying a signal with noise will worsen the scenario due to the noise added by an amplifier. Below, is the analysis of SNR of direct link in comparison with relay link based on

LoS propagation condition [76; 77; 78].

3.2.6.1 Direct Path SNR (gNB-UE):

Referring to Fig 3.6, the received power signal at the destination (UE) using direct path is given by [79]:

$$P_{\mathrm{UE-D}} = \upsilon_{\mathrm{D}}\ P_{\mathrm{gNB}} \tag{3.20}$$

where:

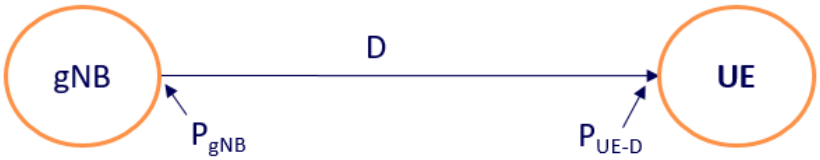

Figure 3.6: Base station to user equipment communication.

- $P_{\mathrm{UE-D}}$ is the UE received power in mW using direct path,
- P_{gNB} is the gNB EIRP transmitted power in mW,
- υ_{D} is the channel gain (coefficient) in the direct link between gNB and UE (including the gains of the antennas at both ends) .

For a typical terrestrial wireless channel, channel gain (coefficient) includes the following effects:

- **Path loss:** Power loss in the signal due to the distance it travels, which is given by Friis formula,
- **Shadowing:** Attenuation/blocking of the signal by large objects like buildings.

The effective SNR i.e ratio of signal power from signal and the noise power is [76; 79]:

$$\mathrm{SNR}_{\mathrm{D-UE}} = \frac{\upsilon_D\ P_{\mathrm{gNB}}}{N_{\mathrm{UE}}} \tag{3.21}$$

where:

- N_{UE} is the noise power picked by destination node.

3.2.6.2 Noise Power

Noise power in a Rx is usually dominated by the thermal noise generated in the frontend Rx amplifier [80]. Thermal noise is also generated in the lossy components of antennas and thermal-like noise is picked up by antennas as radiations from ambient environment. In this case, the

noise power picked by UE can be determined as follows [80]:

$$N_{\mathrm{UE}} = F_{\mathrm{UE}}\ k\ T_o\ B_{\mathrm{UE}} \qquad (mW) \tag{3.22}$$

Where:

- F_{UE} is the UE Rx Noise Figure (NF),
- $k = 1.38 \times 10^{-23}$ J K^{-1} is Boltzmann's constant,
- T_o is the reference Rx temperature, 290°K [81],
- B_{UE} is the UE Rx bandwidth in Hz.

3.2.6.3 Relay Path SNR (gNB-UAV-UE):

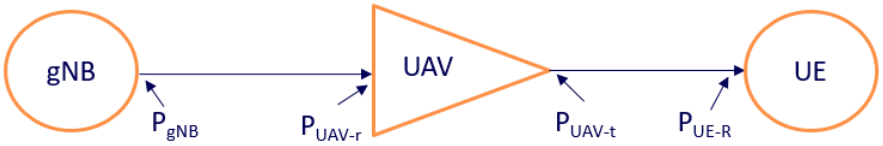

Figure 3.7: gNB To UE communication using a UAV relay node.

Similarly, referring to Fig 3.7, received signal powers at the destination produced by an Amplify-and-Forward relay is given by [79; 80]:

$$\mathrm{P}_{\mathrm{UE-UAV}} = \beta\ \upsilon_1\ \upsilon_2\ P_{\mathrm{gNB}} \tag{3.23}$$

where:

- β is the amplification factor,
- $P_{\mathrm{UAV-r}}$ is the UAV received power in mW,
- υ_1 is the channel gain (coefficient) in the link between gNB and UAV (including the gains of the antennas at both ends).
- υ_2 is the channel gain (coefficient) in the link between UAV and UE (including the gains of the antennas at both ends).

In this case, the noise power picked by the UAV can be determined as follows [80]:

$$N_{\mathrm{UAV}} = F_{\mathrm{UAV}}\ k\ T_o\ B_{\mathrm{UAV}} \qquad (mW) \tag{3.24}$$

Where:

- F_{UAV} is the UE Rx noise figure,
- $k = 1.38 \times 10^{-23}$ J K^{-1} is Boltzmann's constant,
- B_{UAV} is the UE Rx bandwidth in Hz,

The effective SNR is the ratio of signal power from (3.24) , and the noise power which is sum of amplified noise power of UAV relay plus noise power picked up by UE.

$$\mathrm{SNR}_{\mathrm{UE-UAV}} = \frac{\beta\ \upsilon_1\ \upsilon_2\ P_{\mathrm{gNB}}}{\beta\ \upsilon_2\ N_{\mathrm{UAV}} + N_{\mathrm{UE}}} \tag{3.25}$$

3.2.6.4 Relay Path SNR vs Direct Path SNR:

For the relay link to be better in comparison with the direct link, the following inequality should be satisfied.

$$\mathrm{SNR}_{\mathrm{UE-UAV}} > \mathrm{SNR}_{\mathrm{UE}} \tag{3.26}$$

Substituting (3.21) and (3.25) into (3.26) and referring to Fig. 3.8:

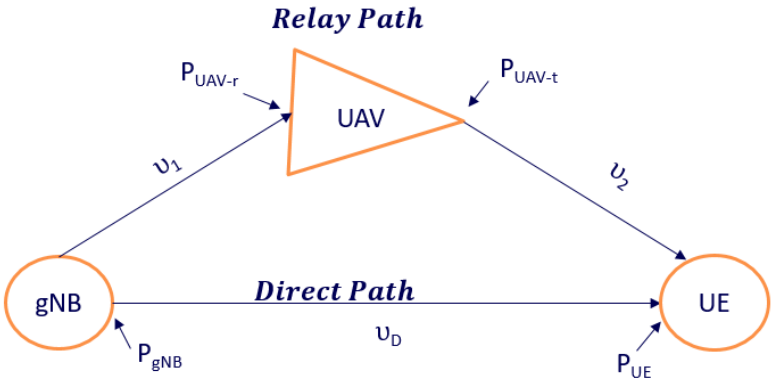

Figure 3.8: Relay Path SNR vs Direct Path SNR.

$$\frac{\beta\ \upsilon_1\ \upsilon_2\ P_{\mathrm{gNB}}}{\beta\ \upsilon_2\ N_{\mathrm{UAV}} + N_{\mathrm{UE}}} > \frac{\upsilon_D\ P_{\mathrm{gNB}}}{N_{\mathrm{UE}}}$$

$$\frac{\beta\ \upsilon_1\ \upsilon_2\ \cancel{P_{\mathrm{gNB}}}}{\beta\ \upsilon_2\ N_{\mathrm{UAV}} + N_{\mathrm{UE}}} > \frac{\upsilon_D\ \cancel{P_{\mathrm{gNB}}}}{N_{\mathrm{UE}}}$$

- **Case 1: With the reasonable assumption of $N_{\mathrm{UE}} = N_{\mathrm{UAV}}$**

$$\frac{\beta\ \upsilon_1\ \upsilon_2}{\cancel{N_{UE}}(\beta\ \upsilon_2\ + 1)} > \frac{\upsilon_D}{\cancel{N_{UE}}}$$

$$\frac{\beta\ \upsilon_1\ \upsilon_2}{\beta\ \upsilon_2 + 1} > \frac{\upsilon_D}{1}$$

$$\beta\ \upsilon_1\ \upsilon_2 > \upsilon_D\ (\beta\ \upsilon_2 + 1)$$

$$\beta\ \upsilon_1\ \upsilon_2 > \upsilon_D\ \beta\ \upsilon_2 + \upsilon_D$$

$$\beta\ \upsilon_1\ \upsilon_2 - \upsilon_D\ \beta\ \upsilon_2 > \upsilon_D$$

$$\beta\ \upsilon_2\ \left(\upsilon_1 - \upsilon_D\right) > \upsilon_D \tag{3.27}$$

It is clear that (3.27) can be satisfied, if $\upsilon_1 > \upsilon_D$. Consequently, with the increase in the amplifier gain the received signal by the UE via the relay path will have eventually more SNR as compared to the direct path.

- **Case 2:** $N_{\mathrm{UE}} \neq N_{\mathrm{UAV}}$

$$\frac{\beta\ \upsilon_1\ \upsilon_2}{N_{\mathrm{UE}}\ \beta\ \upsilon_2 + N_{\mathrm{UAV}}} > \frac{\upsilon_{\mathrm{D}}}{N_{\mathrm{UE}}}$$

$$N_{\mathrm{UE}}\ (\beta\ \upsilon_1\ \upsilon_2) > \upsilon_{\mathrm{D}}\ (N_{\mathrm{UE}}\ \beta\ \upsilon_2 + N_{\mathrm{UAV}})$$

$$N_{\mathrm{UE}}\ \beta\ \upsilon_1\ \upsilon_2 - \upsilon_{\mathrm{D}}\ N_{\mathrm{UE}}\ \beta\ \upsilon_2 > \upsilon_{\mathrm{D}}\ N_{\mathrm{UAV}}$$

$$N_{\mathrm{UE}}\ \beta\ \upsilon_2(\ \upsilon_1 - \upsilon_{\mathrm{D}}) > \upsilon_{\mathrm{D}}\ N_{\mathrm{UAV}}$$

$$\beta\ \upsilon_2(\ \upsilon_1 - \upsilon_{\mathrm{D}}) > \upsilon_{\mathrm{D}}\ \frac{N_{\mathrm{UAV}}}{N_{\mathrm{UE}}} \tag{3.28}$$

Substituting (3.22),and (3.24) into (3.28) :

$$\beta\ \upsilon_2(\ \upsilon_1 - \upsilon_{\mathrm{D}}) > \upsilon_{\mathrm{D}}\ \frac{F_{\mathrm{UAV}}\ k\ T_o\ B_{\mathrm{UAV}}}{F_{\mathrm{UE}}\ k\ T_o\ B_{\mathrm{UE}}} \tag{3.29}$$

It is obvious that (3.29) can be satisfied, if $\upsilon_{\mathrm{D}} > N_{\mathrm{UAV}}/N_{\mathrm{UE}}$. Subsequently, with the increase in the amplifier gain the received signal by the UE via the relay path will have eventually more SNR as compared to the direct path.

The mathematical framework presented in this chapter will be using in the forthcoming chapter for numerical analysis, evaluation and comparison of the mathematical equations with the simulations results.

Chapter 4

Simulations Results, and Discussions

This chapter starts with illustrating simulation using ray-tracing simulator in different urban environments. We present comparison and verification of the simulation results vs mathematical equations (which were presented in chapter 3) i.e., using both analytical approach and ray-tracing simulator results. Furthermore, using ITU recommended city model and based on the propagation conditions i.e., LoS and NLoS , we simulate statistical parameters of the received power in particular; the median and the standard deviation in various urban environments. Additionally, the optimum UAV-gNB height is evaluated in different urban scenarios while providing coverage to the UEs via an Amplify-and-Forward relay. This chapter concludes with the numerical analysis of the SNR for the relay path in comparison with the direct path.

4.1 Ray-Tracing Simulations

In this section, we describe the setup of mmWave channel propagation simulation analysis. Ray-tracing simulations is a method for simulating the propagation of RF signal and has a significant scope in evaluating channel characteristics, and can be used for evaluating novel radio technologies. Ray-tracing methods can provide different parameters like received power, path loss, time delays, angle of arrival, angle of departure, channel impulse response and propagation paths [82]. Received power, and path loss are important for determining system capacity, coverage distances and calculating link budget for cellular system [33]. In contrast to the empirical models or theoretical models which are fast and easy in computation but limited to range-based and mostly valid for the environment where they were developed [83]. In our simulation, we are using Wireless InSite ray-tracing simulator for simulation propagation [84].

4.1.1 Wireless InSite Ray-Tracing Simulator

Wireless InSite® is a suite of ray-tracing models and high-fidelity EM solvers for the analysis of site-specific radio wave propagation and wireless communication systems. The RF propagation software provides efficient and accurate predictions of EM propagation and communication channel characteristics in complex urban, indoor, rural and mixed path environments [84]. Wireless InSite has a unique collection of features that simplifies the analysis of complex and massive propagation problems [83; 84]. Ray-tracing has strong reliance on a number of factors such as the topography, the wavelength, angular steps of the radiating rays, and scattering entities (including vehicles, foliage, and buildings). Fig. 4.1 shows an example of a typical simulation environment setup in Wireless InSite where terrestrial gNB (in green color) is communicating with 8 UAVs (in brown color) and UAV is providing coverage to the ground UEs (in red color).

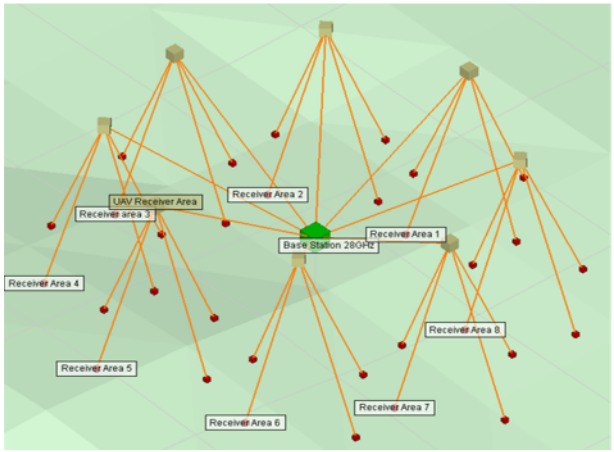

Figure 4.1: Example of Wireless InSite Ray-Tracing simulator: gNB communicating with the UAVs and UAVs providing coverage to the ground UEs

4.1.1.1 Ray-Tracing Simulations Settings

In our ray-tracing simulation, we consider 28 GHz frequency band which is the part of the 5G frequency RF plan [45; 46]. We evaluate and perform our analysis in different simulating scenarios (explained in the coming sections). An isotropic antenna is used for both UAV and ground gNB (at a typical height of 30m) [85]. An isotropic antenna is a theoretical antenna that radiates equally in all directions. The antenna has a gain of 0 dBi and has an efficiency of 100%. The concept of an isotropic antenna is used as a reference antenna for the antenna gain. gNB antenna is feed with a transmit power of +43 dBm (a typical value for lower power macro-cells as per 3GPP) [86], UAV is acting as an Amplify-and-Forward relay with an amplification factor (β) of 50 dB. System and landscape parameter details are stated in Table 4.1. We place 500 UEs uniformly over a disc region of 30m radius from the UAV. Since, this simulation is conducted in free space, so number of reflections, transmission, and diffractions are set to 0. Several simulation

scenarios are performed, described as below:

Table 4.1: Simulation parameters.

Parameter	Value
Frequency	28 GHz
Antenna	Isotropic
Channel Model	Free Space
Number of Reflection	0
Number of Transmissions	0
Number of Diffractions	0
Transmit Power	43 dBm
Number of UEs	500

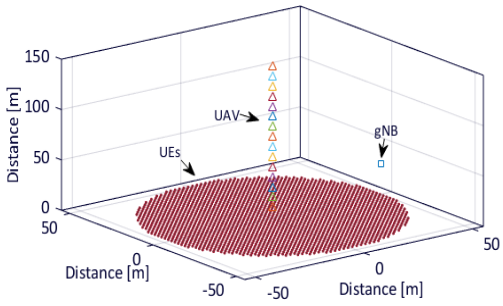

(a) System model

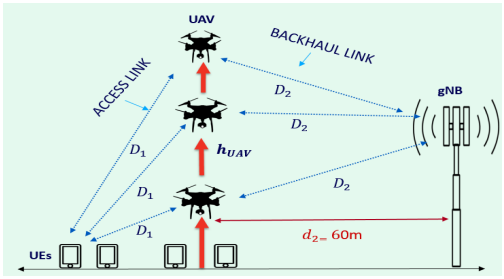

(b) System architecture

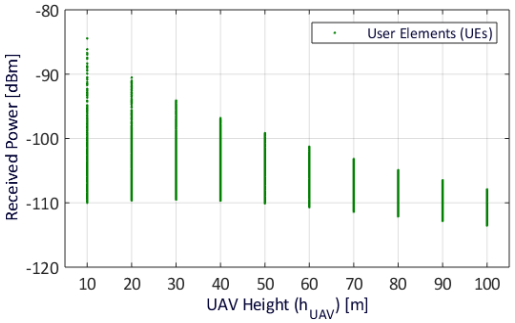

(c) UEs received power vs. UAV height

Figure 4.2: Scenario:1 Variable UAV height

4.1.1.2 Scenario:1 Variable UAV-gNB Height

In this set of simulation, we deploy UAV at horizontal distance of 60m from the gNB with UAV height varied from 10m to 100m. System model and system architecture are shown in Fig. 4.2a, and Fig. 4.2b, respectively. We calculate the received power by UEs via an Amplify-and-Forward relay (UAV) and results are depicted in Fig. 4.2. We observe that as the UAV height increases, the received power by the UEs decreases and most number of UEs are receiving good coverage when the UAV height is at 30m (which is the same height of the gNB). Likewise, we notice that

edge users coverage is optimum at this point. Additionally, we observe that with the increase in the UAV height, the level of the received power by the UEs decreases.

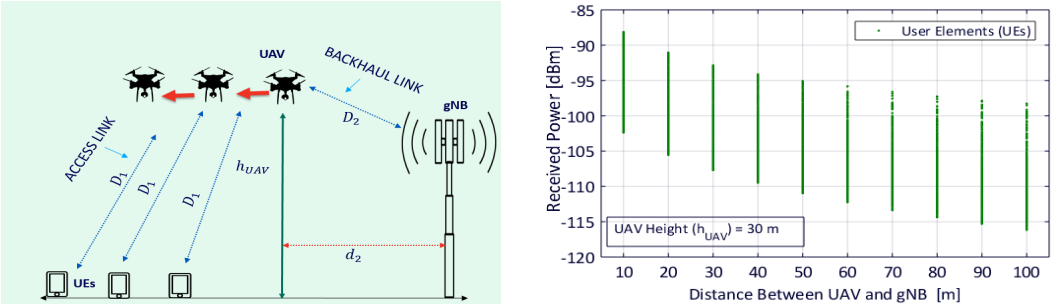

(a) System architecture

(b) UEs received power vs. UAV to gNB distance

Figure 4.3: Scenario:2 Variable UAV horizontal distance

4.1.1.3 Scenario:2 Variable UAV-gNB Horizontal Distance

In this set of simulation, we deploy UAV at a fixed height of 30m (same height as the gNB) and move UAV in a horizontal direction (away) from the gNB, depicted in Fig. 4.3a. We calculate the received power by the UEs via the Amplify-and-Forward relay (UAV) and results are depicted in Fig. 4.3b. We observe that as the distance between the UAV and gNB increases, the received power the by UEs decreases. Hence, in this case, the nearest point with the gNB will be the optimum point (if applicable).

4.1.1.4 Scenario:3 Variable UAV-gNB Height and Horizontal Distance

In this set of simulation, we preform the analysis by varying both the UAV elevation and the UAV horizontal distance. We deploy UAV at a horizontal distance of 20m, 40m and 60m from the gNB, respectively. For each horizontal distance, we elevate the UAV from 10m to 100m, as depicted in Fig. 4.4. We calculate the received power by UEs via the Amplify-and-Forward relay (UAV) and results are shown in Fig. 4.4. We observe that as the UAV height increases, the received power by the UEs decreases and most number of UEs are receiving good coverage when the UAV height is at 30m (which is the same height of the gNB). Likewise, we notice that edge users coverage is optimum at this point.

4.2 Models Comparison and Verification

In this section, we present comparison and verification of the simulation results vs mathematical equations (which were presented in chapter 3). Mathematical propagation models simplify the calculations and speed up radio coverage estimations. Similarly, deterministic ray-tracing models are shown to be most accurate if the relevant parameters and description (environment

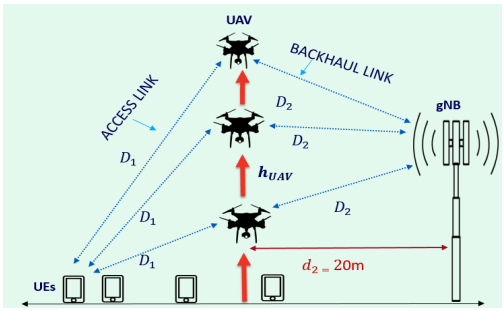

(a) Simulation Scenario:1

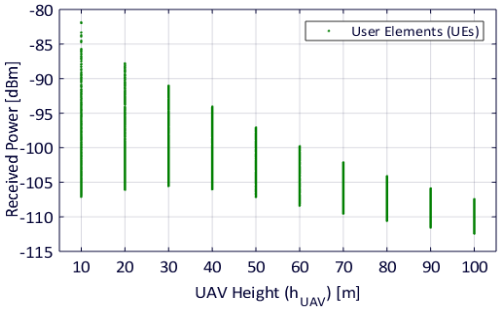

(b) $d_2 = 20m$

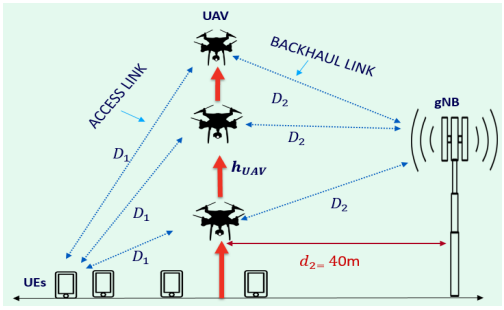

(c) Simulation Scenario:2

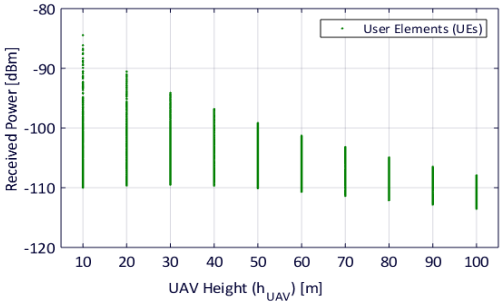

(d) $d_2 = 40m$

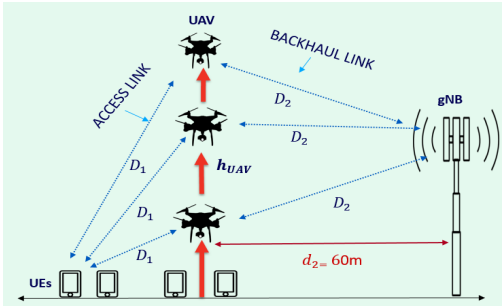

(e) Simulation Scenario:3

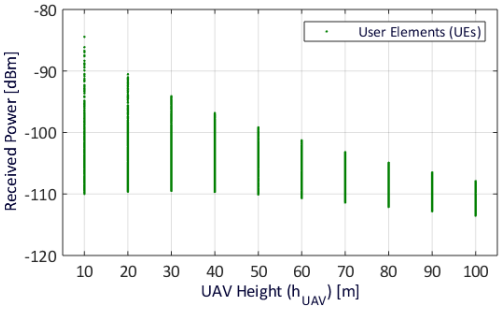

(f) $d_2 = 60m$

Figure 4.4: Scenario 3: UAV vertical and horizontal movement.

details, building databases etc.) are properly feed to it; though high computation time and operation complexity has hindered its widespread applications. For this purpose, we consider the scenario, depicted in Fig.4.5a, where terrestrial gNB is communicating with UAV and UAV is providing coverage to the ground UEs. We use 28 GHz frequency band for both links (Access and Backhaul). Furthermore, an isotropic antenna is deployed both at gNB and UAV and we feed gNB with a transmit power of 43 dBm. We deploy UAV at horizontal distance of 60m from the gNB, and UAV was elevated from 10m to 100m. We calculate received power by UEs using two methods:

- Friis Transmission Equation (Eq. 3.8), and
- Wireless InSite Ray-Tracing Simulator(Free Space).

We illustrate results in Fig. 4.5b, Fig. 4.5c, and it is visible that received power by the UEs

via Friis Transmission Equation, and Wireless In Site simulations is following exactly the same trend trend. Moreover, in Fig. 4.5d, we depict the comparison of both the Friis Transmission Equation and Wireless In Site simulations results.

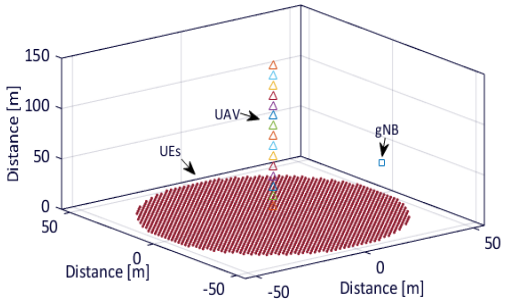

(a) System model

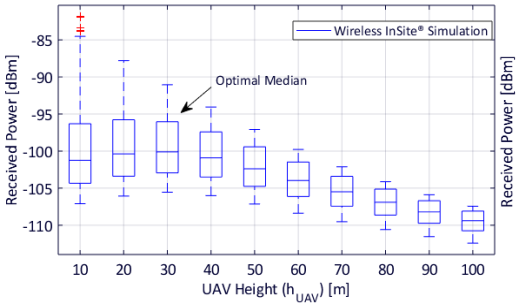

(b) Wireless InSite simulation

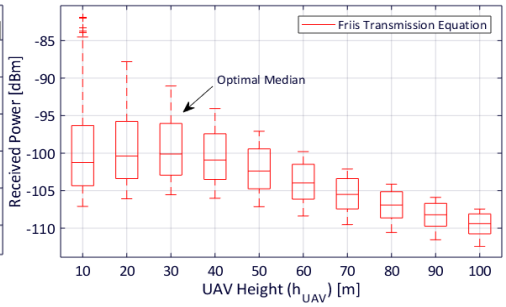

(c) Friis Transmission Equation via Matlab

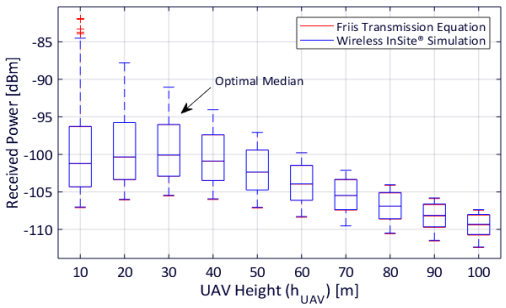

(d) Comparison of Friis Transmission Equation and simulation results

Figure 4.5: Model verification and comparison.

4.3 Direct Path Vs Relay Path Evaluation

As highlighted earlier, UAV utilization as an Amplify-and-Forward relay is beneficial in providing coverage to the shadowed zones and enhancing capacity as well. In this section, we evaluate the performance of the direct path (between the gNB and UE) and the relay path (between the gNB and UE via UAV) with a variable amplification factor (β) by considering the scenario depicted in Fig.4.6a, where a terrestrial gNB is communicating with the UAV and UAV is providing coverage to the ground UE. We use 28 GHz frequency band for both the links (Access and

Backhaul). Furthermore, an isotropic antenna is used for both at gNB (at a typical height of 30m) and the ground UE (at a height of 1.5m) [85]. For the UAV, parabolic antenna is deployed with a gain of 23 dBi at the receiving end. The UE is positioned at a distance of 50m from the UAV and UAV is deployed at a distance of 40m from the gNB. Terrestrial BS is feed with a transmit power of +43 dBm. For the sake of simplicity, we only considered losses of free space path losses. We calculate the UE received power via direct and relay paths using (3.12) by varying the amplification factor (β) from 20 dB to 80 dB, and results are depicted in Fig. 4.6b. From the results, it is obvious that a suitable amplification factor is required in UAV for achieving better signal strength in the relay path with comparison to the direct path.

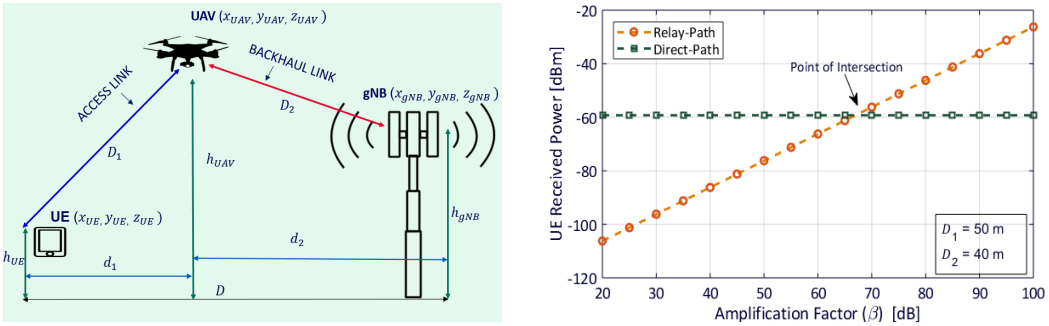

(a) Simulation Scenario

(b) Amplification factor (β) vs. received power

Figure 4.6: Received power of direct path vs. relay path

4.4 Evaluation of LoS and NLoS Scenarios

In wireless communication networks, distinguishing between LoS and NLoS link status is of high importance. LoS communication links can potentially leads to significant performance improvement as compare to NLoS links, especially in the emerging mmWave communications [21]. Statistical parameters varies accordingly and earlier characterization of LoS and NLoS links can facilitate in accurate channel modelling and will ultimately lead to more reliable channel assessments, especially in the UAV-relay networks. In chapter 3, LoS probability is plotted for different urban environments in Fig. 3.5 based on (3.15), (which are derived in chapter 3). In this section, we calculate the mean received power by UEs in different urban environments, while segregating LoS and NLoS modes. We build the system model via Matlab programming language, where we uniformly distribute UEs at an equal distance of 2m within a disc region of radius 50m with a height of 1.5m. A terrestrial gNB is deployed at a height of 30m with a horizontal distance of 40m from the UAV. We vary the UAV height from 10m to 100m by considering different urban environments based on ITU-R recommendation city model. Since, there are two links: (i) gNB to UAV, and (ii) UAV to UE; gNB to UAV link is assumed LoS and for UAV to UE link, we utilize probabilities based on (3.15). For obtaining the LoS condition, we realize a Bernoulli random

variable for each UE with a success probability of $\mathrm{P(LoS)_{UAV-UE}}$. The Bernoulli Distribution is a discrete distribution having two possible outcomes: either success or failure, as explained by the below function:

$$\mathrm{rand(length(P(LoS)_{UAV-UE}), 1)} < \mathrm{P(LoS)_{UAV-UE}}$$

where:

- $\mathrm{P(LoS)_{UAV-UE}}$ is the LoS probability for UE, referring to (3.15),
- The rand function generates arrays of random numbers whose elements are uniformly distributed in the interval ((length($\mathrm{P(LoS)_{UAV-UE}}$),1).

gNB link is considered LoS, and for UAV to UE LoS link, probability for different environments is calculated for each UE based on its elevation angle, as below [5; 33]:

$$d_1 = \frac{h_{\mathrm{UE}}}{\tan(\theta)}$$

where:

- θ is the UE elevation angle with UAV,
- d_1 is the horizontal distance between UE and UAV.

4.4.1 Suburban Environment

We started our analysis with suburban environment which has the following parameters [5], depicted in Fig. 4.7:

- Ratio of built-up land area to the total land area, A: 0.1,
- Mean number of building per unit area, B_1: 750,
- Buildings $'$ heights distribution, C: 8.

We calculate the mean received power of the UEs and plot it in Fig. 4.7. In suburban environment building concentration is less which results in increase in probability of LoS rays concentration. We record that the optimal UAV height is in the same range as the gNB height. We also highlight the UEs which are getting LoS coverage (in red colour) and the UEs, which are getting NLoS coverage (in blue colour) in Fig. 4.7.

4.4.2 Urban Environment

Subsequently, we consider an urban environment which has the following parameters [5], depicted in Fig. 4.8:

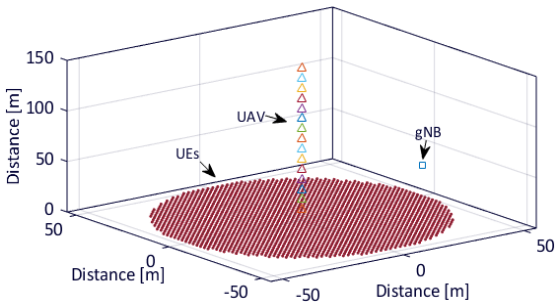

(a) System model

(b) Suburban environment(A: 0.1, B_1: 750, C: 8)

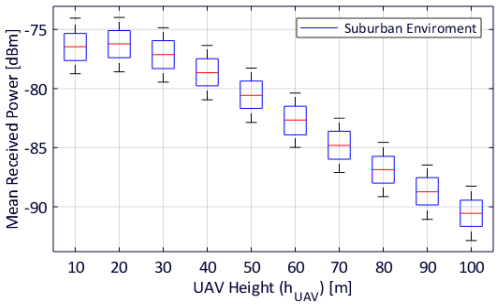

(c) Mean received power for suburban environment

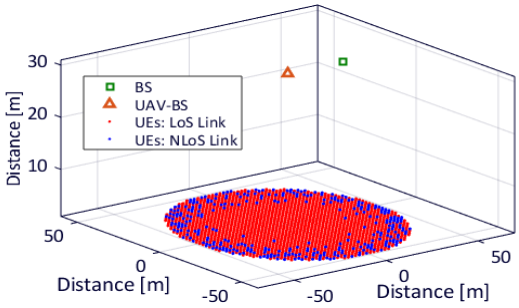

(d) UEs segregation into LoS and NLoS modes

Figure 4.7: Suburban environment.

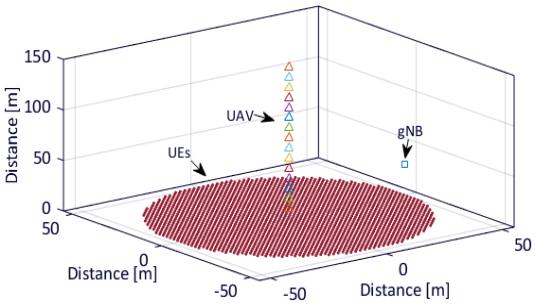

(a) System model

(b) Urban environment(A: 0.3, B_1: 500, C: 15)

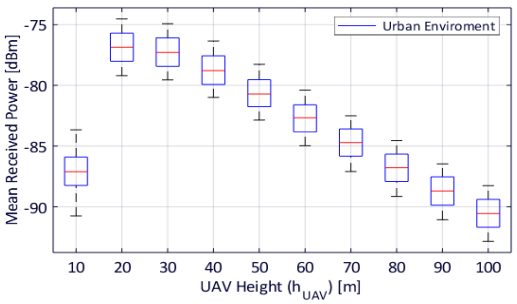

(c) Mean received power for urban environment

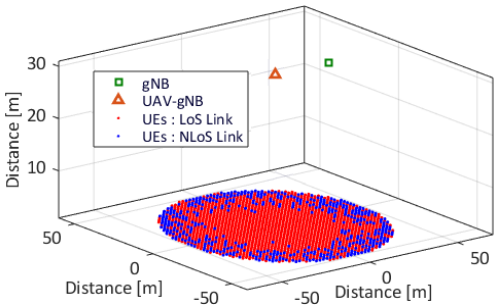

(d) UEs segregation into LoS and NLoS modes

Figure 4.8: Urban Environment.

- Ratio of built-up land area to the total land area, A: 0.3,
- Mean number of building per unit area, B_1: 500,

- Buildings ′ heights distribution, C: 15.

The mean received power of the UEs is calculated and plotted in Fig. 4.8. From the charts, it is visible that the optimal UAV height is in the same range as the gNB height. Similarly, the UEs which are getting LoS coverage are highlighted in red colour and the UEs which are getting NLoS coverage are shown in blue colour in Fig. 4.8.

4.4.3 Dense Urban Environment

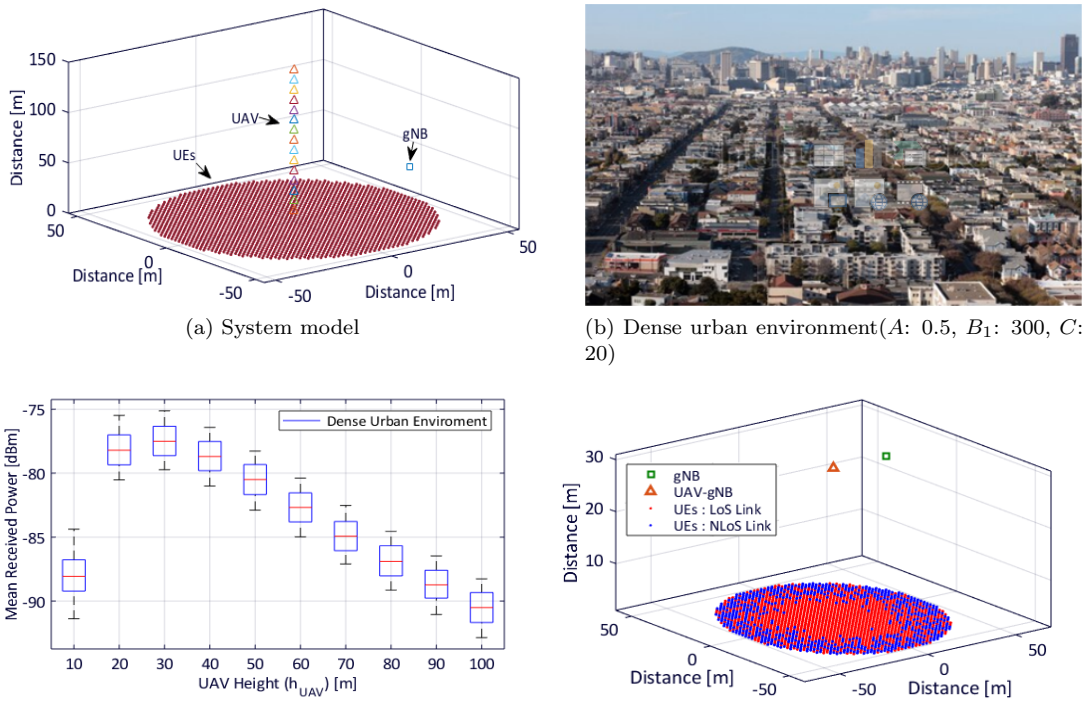

(a) System model

(b) Dense urban environment(A: 0.5, B_1: 300, C: 20)

(c) Mean received power for dense urban environment

(d) UEs Segregation into LoS and NLoS modes

Figure 4.9: Dense urban environment.

Afterwards, the same analysis is performed for the dense urban environment which has the following parameters [5], depicted in Fig. 4.9:

- Ratio of built-up land area to the total land area, A: 0.5,
- Mean number of building per unit area, B_1: 300,
- Buildings ′ heights distribution, C: 20,

We calculate the mean received power of the UEs and plot it in Fig. 4.9. We notice that the optimal UAV height in the dense urban environment is the same range as the gNB height. We also depict the UEs which are getting LoS coverage (in red colour) and the UEs, which are getting NLoS coverage (in blue colour) in Fig. 4.9.

4.4.4 High-Rise Urban Environment

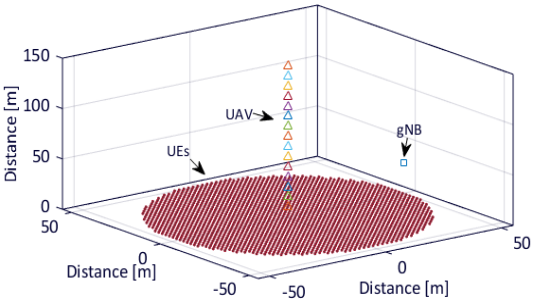

(a) System model

(b) High-rise urban environment(A: 0.5, B_1: 300, C: 50)

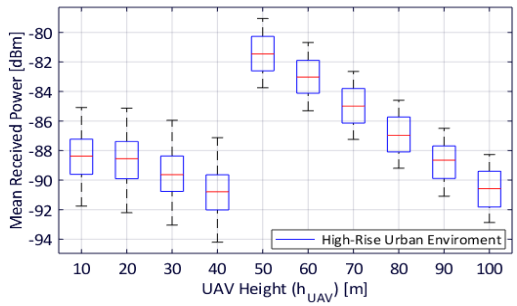

(c) Mean received power for high-rise urban enviroment

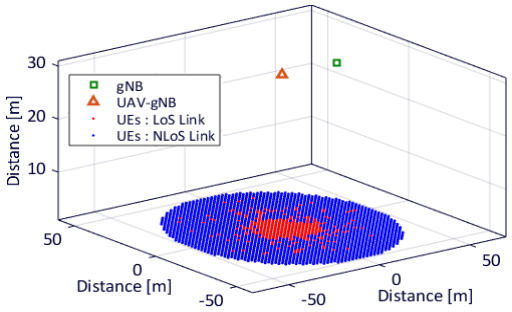

(d) UEs Segregation into LoS and NLoS modes

Figure 4.10: Urban environments

Finally, we perform the analysis and investigation for the high-rise urban environment which has the following parameters [5], depicted in Fig. 4.10:

- Ratio of built-up land area to the total land area, A: 0.5,
- Mean number of building per unit area, B_1: 300,
- Buildings $'$ heights distribution, C: 50,

The mean received power of the UEs is calculated and plotted in Fig. 4.10. In high rise urban environments concatenation of building is more so UAV has to be elevated more to get the optimal position. Similarly, we highlight the UEs which are getting LoS coverage (in red colour) and the UEs, which are getting NLoS coverage (in blue colour) in Fig. 4.10. It is obvious, that the lesser number of UEs are in the LoS coverage as compare to the urban and suburban environments.

The LoS probability corresponds to the probability that the signal from transmitter to receiver will reach along an unobstructed propagation path i.e. zero reflection or scattering which indicates the absence of obstacles in the communicating path. However, minimum UAV height is more to prone to be obstructed which should be considered in the channel assessments and network deployments in different urban environments.

In contrary to the lower frequencies, the key challenge in mmWave band is the high increase in the path loss with the growing distance between Tx and Rx, which is a trade-off between placing UAV at higher altitude and providing quality LoS links while maintaining minimal path loss [3]. Since, UAV will be elevated more to get the optimum coverage in high rise urban environment which also replicate that coverage radius for suburban area will be greater than high rise urban environment.

4.5 SNR Analysis: Direct Path Vs Relay Path: LoS Propagation Condition

In this section, we present the numerical analysis of the SNR for the relay path in comparison with the direct path. We deploy a UAV at a horizontal distance of 50m from the gNB and position the UE at a distance of 100m and 60m from gNB and UAV, respectively as depicted in Fig. 4.11. Terrestrial gNB is feed with a transmit power of +43 dBm [86]. An isotropic antenna is used for both the gNB (at a typical height of 30m) and the ground UE (at a height of 1.5m) [85]. An isotropic antenna is a theoretical antenna that radiates equally in all directions and has a gain of 0 dBi with an efficiency of 100%. For the UAV, we deploy parabolic antenna with a gain of 23 dBi at the receiving end. For the sake of simplicity, we only considered the losses of free space path losses. The noise power of the UAV and UE receivers are considered as -106 dBm and -104 dBm, respectively [87]. We calculate and plot the SNR of the direct and the relay paths against varying amplification factor (β), illustrated in Fig. 4.11. The SNR of direct path is constant, however, at the point of intersection the SNR of the relay path is better than direct path. Therefore, in this scenario, as the amplifier gain increases, the received power via relay will have eventually more SNR as compare to direct path.

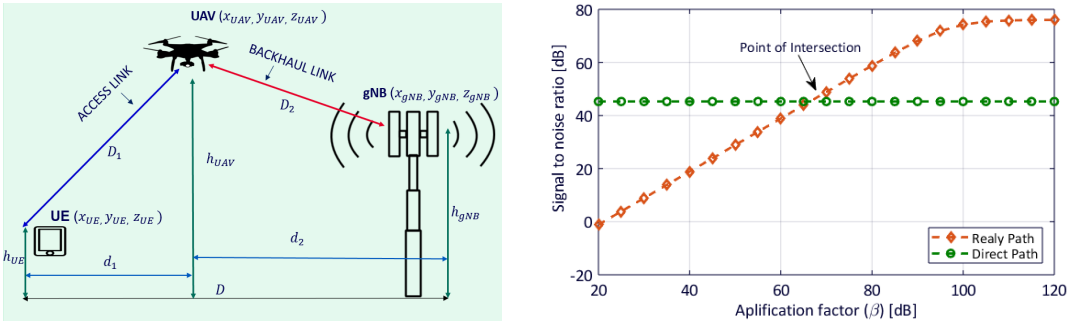

(a) Simulation scenario

(b) Amplification factor vs. received power

Figure 4.11: Results of SNR of direct path vs. relay paths

Chapter 5

Conclusions and Future Work

The utilization of mmWave band has a huge potential in the next generation wireless networks because of vast available bandwidth and the pencil beam high gain antenna arrays. However, its sensitivity to blockage is a restraining factor, which is causing considerable signal strength variability between LoS and NLoS conditions. The architecture presented in this study provides a promising solution to the above problems through UAV (allowing for aerial-to-ground LoS link, and a controllable movement in 3D space). The goal of this study was the evaluation of the performance of next generation UAV networks using mmWave in Access and Backhaul links. In this study, the mathematical framework and ray-tracing simulation presents in-depth details and multi-path propagation, permitting assessment of how the environment and the placement of communication nodes impact system performance. The optimum UAV-gNB height is evaluated in different urban scenarios while providing coverage to the UEs via an Amplify-and-Forward relay which is very beneficial for planning and deployment of UAV-gNB assisted network especially in the upcoming smart cities.

5.1 Summary of RQ1 Outcomes

The main observations and outcomes of RQ1 can be summarized as following:
(refer to Chapter 3 for details)

- We derived a mathematical framework, having equations for calculating the UE received power:
    1. For direct path (gNB-UE) using Friis Transmission Equation,
    2. For relay path (gNB-UAV-UE) using Friis Transmission Equation,
    3. For direct path ((gNB-UE) using Log-Distance path loss model (shadowing),
    4. For relay path (gNB-UAV-UE) using Log-Distance path loss model (shadowing),
- We utilized the probability for LoS and NLoS paths in different urban environments for the proposed system architecture using ITU recommended city model,

- We performed the SNR analysis of the relay path in comparison with the direct path and highlighted the related constraints,

5.2 Summary of RQ2 outcomes

The main observations and outcomes of RQ2 can be summarised as following:

- We compared and verified the simulation results against the presented mathematical framework to validate both the model and the simulations results,
- We performed ray-tracing simulation in different scenarios to evaluate the performance of an Amplify-and-Forward UAV relay in free space and different urban environments,
- We explored, evaluated and analyzed different parameters i.e., UAV-gNB location, and amplification factor to maximise the performance of an Amplify-and-Forward UAV relay for providing enhanced coverage area. Evaluation of UAV optimum height was conducted in different urban environments,
- Furthermore, the need of suitable amplification factor was highlighted (in the UAV-gNB) for having better signal strength in the relay path with comparison to the direct path,
- At the end, we performed numerical analysis of the SNR for the relay path in comparison with the direct path.

5.3 Final Remarks and Future Directions

In this thesis, we conclude that ray-tracing simulator facilitates in planning of coverage and understanding key propagation parameters. We derive a mathematical framework with the goal to investigate and evaluate the use of mmWave in Access and Back-haul communication links simultaneously for an Amplify-and-Forward relay deployed on UAVs. For the future work, we plan to use machine learning algorithms for optimizing the deployment of UAV-gNB in 3D space, identifying propagation environment features such as mountains, ridges, rural areas, cities and determining appropriate level of details to the respective environmental model. Additionally, in cellular communication industry perspective, using mmWave for cellular coverage is a a key concern. We plan to extend our study using MIMO antennas in the UAV-gNB. Large antenna arrays can permit for compensation of severe propagation conditions at high frequency [88; 89].

References

[1] M. Iwamura, H. Takahashi, and S. Nagata, "Relay technology in lte-advanced," *NTT DoCoMo Technical Journal*, vol. 12, no. 2, pp. 29–36, 2010. 8, 10, 18, 19, 26, 30

[2] Huawei, *Policy Report*, http://www-file.huawei.com/-/media/CORPORATE/PDF/public-policy/public_policy_position_5g_spectrum.pdf, 2016. 8, 21

[3] S. Sun, T. S. Rappaport, T. A. Thomas, A. Ghosh, H. C. Nguyen, I. Z. Kovács, I. Rodriguez, O. Koymen, and A. Partyka, "Investigation of prediction accuracy, sensitivity, and parameter stability of large-scale propagation path loss models for 5g wireless communications," IEEE Transactions on Vehicular Technology, vol. 65, no. 5, pp. 2843–2860, 2016. 10, 24, 51

[4] S. Sun, T. S. Rappaport, M. Shafi, P. Tang, J. Zhang, and P. J. Smith, "Propagation models and performance evaluation for 5g millimeter-wave bands," *IEEE Transactions on Vehicular Technology*, vol. 67, no. 9, pp. 8422–8439, 2018. 10, 24

[5] ITU, *Propagation data and prediction methods required for the design of terrestrial broadband millimetric radio access systems operating in a frequency range of about 20-50 GHz*, 2003. 10, 33, 34, 47, 49, 50

[6] ITU, *Release-15 3rd Generation Partnership Project (3GPP)*, https://www.3gpp.org/release-15,2019. 2, 21

[7] Y. Chen, W. Feng, and G. Zheng, "Optimum placement of uav as relays," *IEEE Communications Letters*, vol. 22, pp. 248–251, Feb 2018. 2, 21

[8] Cicso, *"Cisco visual networking Index*, https://www.cisco.com/c/dam/en/us/solutions/collateral/service-provider/visual-networking-index-vni/complete-white-paper-c11-481360.pdf,2017. 2

[9] S. Kutty and D. Sen, "Beamforming for millimeter wave communications: An inclusive survey," *Communications Surveys, Tutorials, IEEE*, vol. 18, no. 2, pp. 949–973, 2016. 2

[10] Y. Niu, Y. Li, D. Jin, L. Su, and A. V. Vasilakos, "A survey of millimeter wave communications (mmwave) for 5g: opportunities and challenges," *Wireless Networks*, vol. 21, pp. 2657–2676, Nov 2015. 2

[11] A. V. Linghe Kong, A. V. Linsheng Ye, A. V. Fan Wu, A. V. Meixia Tao, A. V. Guihai Chen, and A. V. Vasilakos, "Autonomous relay for millimeter-wave wireless communications," *Selected Areas in Communications, IEEE Journal on*, vol. 35, no. 9, pp. 2127–2136, 2017. 2

[12] M. Akdeniz, Y. Liu, M. Samimi, S. Sun, S. Rangan, T. Rappaport, and E. Erkip, "Millimeter wave channel modeling and cellular capacity evaluation," *IEEE Journal on Selected Areas in Communications*, vol. 32, no. 6, pp. 1164–1179, 2014. 2

[13] *"LTE Unmanned Aircraft Systems Trial Report1*, https://www.qualcomm.com/documents/lte-unmanned-aircraft-systems-trial-repor, 2017. 2

[14] X. Lin, V. Yajnanarayana, S. D. Muruganathan, S. Gao, H. Asplund, H. Maattanen, M. Bergstrom, S. Euler, and Y. . E. Wang, "The sky is not the limit: Lte for unmanned aerial vehicles," *IEEE Communications Magazine*, vol. 56, pp. 204–210, APRIL 2018. 2

[15] Q. Wu, J. Xu, and R. Zhang, "Capacity characterization of uav-enabled two-user broadcast channel," *CoRR*, vol. abs/1801.00443, 2018. 3

[16] L. Kong, L. Ye, F. Wu, M. Tao, G. Chen, and A. V. Vasilakos, "Autonomous relay for millimeter-wave wireless communications," *IEEE Journal on Selected Areas in Communications*, vol. 35, pp. 2127–2136, Sept 2017. 3

[17] *Facebook Technical Report*, https://fbnewsroomus.files.wordpress.com/2014/03/connecting-the-world-from-the-sky1.pdf,2004. 3

[18] A. govt, *Regulation of Drones: Australia*, ,https://www.loc.gov/law/help/regulation-of-drones/australia.php,2016. 3

[19] M. Alzenad, A. El-Keyi, F. Lagum, and H. Yanikomeroglu, "3-d placement of an unmanned aerial vehicle base station (uav-bs) for energy-efficient maximal coverage," *IEEE Wireless Communications Letters*, vol. 6, no. 4, pp. 434–437, 2017. 3, 19

[20] M. Mozaffari, W. Saad, M. Bennis, Y. Nam, and M. Debbah, "A tutorial on uavs for wireless networks: Applications, challenges, and open problems," *CoRR*, vol. abs/1803.00680, 2018. 3, 4

[21] Y. Zeng, R. Zhang, and T. J. Lim, "Wireless communications with unmanned aerial vehicles: opportunities and challenges," *IEEE Communications Magazine*, vol. 54, pp. 36–42, May 2016. 3, 46

[22] M. Xiao, S. Mumtaz, Y. Huang, L. Dai, Y. Li, M. Matthaiou, G. K. Karagiannidis, E. Björnson, K. Yang, I. Chih-Lin, *et al.*, "Millimeter wave communications for future mobile networks," *IEEE Journal on Selected Areas in Communications*, vol. 35, no. 9, pp. 1909–1935, 2017. 4

[23] Y. Dong, M. Z. Hassan, J. Cheng, M. J. Hossain, and V. C. M. Leung, "An edge computing empowered radio access network with uav-mounted FSO fronthaul and backhaul: Key challenges and approaches," *CoRR*, 2018. 4, 10, 11

[24] Y. Zeng, R. Zhang, and T. J. Lim, "Wireless communications with unmanned aerial vehicles: opportunities and challenges," *IEEE Communications Magazine*, vol. 54, pp. 36–42, May 2016. 9, 10, 20

[25] J. Kakar and V. Marojevic, "Waveform and spectrum management for unmanned aerial systems beyond 2025," *CoRR*, 2017. 10, 11

[26] T. Yang, F. Song, X. Chen, Y. Zhang, and K. Yao, "Demand-aware backhaul allocation in uav networks: A stackelberg optimization approach," pp. 378–383, Dec 2017. 10, 12

[27] F. Ahdi and S. Subramaniam, "Using unmanned aerial vehicles as relays in wireless balloon networks," pp. 3795–3800, June 2015. 10, 12

[28] J. Bartelt, P. Rost, D. Wubben, J. Lessmann, B. Melis, and G. Fettweis, "Fronthaul and backhaul requirements of flexibly centralized radio access networks," *IEEE Wireless Communications*, vol. 22, pp. 105–111, October 2015. 10, 13

[29] P.-H. Kuo and A. Mourad, "Millimeter wave for 5g mobile fronthaul and backhaul," pp. 1–5, June 2017. 10, 13

[30] R. J. Weiler, M. Peter, W. Keusgen, E. Calvanese-Strinati, A. D. Domenico, I. Filippini, A. Capone, I. Siaud, A. M. Ulmer-Moll, A. Maltsev, T. Haustein, and K. Sakaguchi, "Enabling 5g backhaul and access with millimeter-waves," pp. 1–5, June 2014. 10, 14

[31] F. Boccardi, H. Shokri-Ghadikolaei, G. Fodor, E. Erkip, C. Fischione, M. Kountouris, P. Popovski, and M. Zorzi, "Spectrum pooling in mmwave networks: Opportunities, challenges, and enablers," *IEEE Communications Magazine*, vol. 54, pp. 33–39, November 2016. 10, 14

[32] S. A. R. Naqvi, S. A. Hassan, H. Pervaiz, and Q. Ni, "Drone-aided communication as a key enabler for 5g and resilient public safety networks," *IEEE Communications Magazine*, vol. 56, pp. 36–42, Jan 2018. 10, 15

[33] A. Al-Hourani, S. Kandeepan, and A. Jamalipour, "Modeling air-to-ground path loss for low altitude platforms in urban environments," pp. 2898–2904, Dec 2014. 10, 15, 19, 33, 34, 40, 47

[34] V. Sharma, R. Sabatini, and S. Ramasamy, "Uavs assisted delay optimization in heterogeneous wireless networks," *IEEE Communications Letters*, vol. 20, no. 12, pp. 2526–2529, 2016. 17, 20

[35] Q. Plessis, M. Suzuki, T. Kitahara, and S. Ano, "Group mobility in mobile networks: Signaling based detection and network utilization modeling," in *2016 IEEE Global Communications Conference (GLOBECOM)*, pp. 1–7, IEEE, 2016. 17

[36] A. Colpaert, E. Vinogradov, and S. Pollin, "Aerial coverage analysis of cellular systems at lte and mmwave frequencies using 3d city models," *Sensors*, vol. 18, no. 12, p. 4311, 2018. 17

[37] J. N. Laneman, D. N. Tse, and G. W. Wornell, "Cooperative diversity in wireless networks: Efficient protocols and outage behavior," *IEEE Transactions on Information theory*, vol. 50, no. 12, pp. 3062–3080, 2004. 17

[38] M. Mozaffari, W. Saad, M. Bennis, and M. Debbah, "Unmanned aerial vehicle with underlaid device-to-device communications: Performance and tradeoffs," *IEEE Transactions on Wireless Communications*, vol. 15, no. 6, pp. 3949–3963, 2016. 19

[39] M. Mozaffari, W. Saad, M. Bennis, and M. Debbah, "Efficient deployment of multiple unmanned aerial vehicles for optimal wireless coverage," *IEEE Communications Letters*, vol. 20, no. 8, pp. 1647–1650, 2016. 19

[40] M. M. Azari, F. Rosas, K.-C. Chen, and S. Pollin, "Optimal uav positioning for terrestrial-aerial communication in presence of fading," in *2016 IEEE Global Communications Conference (GLOBECOM)*, pp. 1–7, IEEE, 2016. 20

[41] E. Yanmaz, "Connectivity versus area coverage in unmanned aerial vehicle networks," in *2012 IEEE International Conference on Communications (ICC)*, pp. 719–723, IEEE, 2012. 20

[42] E. Kalantari, M. Z. Shakir, H. Yanikomeroglu, and A. Yongacoglu, "Backhaul-aware robust 3d drone placement in 5g+ wireless networks," in *2017 IEEE International Conference on Communications Workshops (ICC Workshops)*, pp. 109–114, IEEE, 2017. 20

[43] S. Parkvall, E. Dahlman, A. Furuskar, and M. Frenne, "Nr: The new 5g radio access technology," *IEEE Communications Standards Magazine*, vol. 1, no. 4, pp. 24–30, 2017. 21

[44] F. Qamar, M. H. S. Siddiqui, K. Dimyati, K. A. B. Noordin, and M. B. Majed, "Channel characterization of 28 and 38 ghz mm-wave frequency band spectrum for the future 5g network," in *2017 IEEE 15th student conference on research and development (SCOReD)*, pp. 291–296, IEEE, 2017. 21

[45] S. Rangan, T. S. Rappaport, and E. Erkip, "Millimeter-wave cellular wireless networks: Potentials and challenges," *Proceedings of the IEEE*, vol. 102, pp. 366–385, March 2014. 21, 41

[46] W. R. C. Conference, *Provisional Final Acts World Radio communication Conference (WRC-15)*, 2015. 21, 41

[47] Y. Huo, X. Dong, and J. Bornemann, "A wideband artificial magnetic conductor yagi antenna for 60-ghz standard 0.13-μm cmos applications," in *2014 12th IEEE International Conference on Solid-State and Integrated Circuit Technology (ICSICT)*, pp. 1–3, IEEE, 2014. 22

[48] M. Mozaffari, W. Saad, M. Bennis, Y.-H. Nam, and M. Debbah, "A tutorial on uavs for wireless networks: Applications, challenges, and open problems," *IEEE Communications Surveys & Tutorials*, 2019. 22, 33

[49] R. I. Bor-Yaliniz, A. El-Keyi, and H. Yanikomeroglu, "Efficient 3-d placement of an aerial base station in next generation cellular networks," in *2016 IEEE international conference on communications (ICC)*, pp. 1–5, IEEE, 2016. 22, 25, 33

[50] M. Mozaffari, W. Saad, M. Bennis, and M. Debbah, "Drone small cells in the clouds: Design, deployment and performance analysis," in *2015 IEEE Global Communications Conference (GLOBECOM)*, pp. 1–6, IEEE, 2015. 22, 25, 33

[51] 3GPP, *The Mobile Broadband Standard,*, https://www.3gpp.org/release-15, 2018. 22, 25, 33

[52] Y. Zhu, G. Zheng, and M. Fitch, "Secrecy rate analysis of uav-enabled mmwave networks using matérn hardcore point processes," *IEEE Journal on Selected Areas in Communications*, vol. 36, no. 7, pp. 1397–1409, 2018. 22

[53] T. Bai and R. W. Heath, "Coverage and rate analysis for millimeter-wave cellular networks," *IEEE Transactions on Wireless Communications*, vol. 14, no. 2, pp. 1100–1114, 2014. 22

[54] D. Maamari, N. Devroye, and D. Tuninetti, "Coverage in mmwave cellular networks with base station co-operation," *IEEE Transactions on Wireless Communications*, vol. 15, no. 4, pp. 2981–2994, 2016. 22

[55] W. Yi, Y. Liu, and A. Nallanathan, "Modeling and analysis of d2d millimeter-wave networks with poisson cluster processes," *IEEE Transactions on Communications*, vol. 65, no. 12, pp. 5574–5588, 2017. 22

[56] W. Yi, Y. Liu, E. Bodanese, A. Nallanathan, and G. K. Karagiannidis, "A unified spatial framework for uav-aided mmwave networks," *arXiv preprint arXiv:1901.01432*, 2019. 22

[57] M. Gapeyenko, I. Bor-Yaliniz, S. Andreev, H. Yanikomeroglu, and Y. Koucheryavy, "Effects of blockage in deploying mmwave drone base stations for 5g networks and beyond," in *2018 IEEE International Conference on Communications Workshops (ICC Workshops)*, pp. 1–6, May 2018. 22

[58] Y. Azar, G. N. Wong, K. Wang, R. Mayzus, J. K. Schulz, H. Zhao, F. Gutierrez Jr, D. Hwang, and T. S. Rappaport, "28 ghz propagation measurements for outdoor cellular communications using steerable beam antennas in new york city.," in *ICC*, pp. 5143–5147, 2013. 23, 29

[59] S. Deng, M. K. Samimi, and T. S. Rappaport, "28 ghz and 73 ghz millimeter-wave indoor propagation measurements and path loss models," in *2015 IEEE International Conference on Communication Workshop (ICCW)*, pp. 1244–1250, IEEE, 2015. 23, 29

[60] R. Tahri, S. Collonge, G. Zaharia, and G. Zein, "Spatial characterization of 60 ghz indoor channels by fast gaussian beam tracking method and comparison with measurements," in *2006 IEEE 63rd Vehicular Technology Conference*, vol. 6, pp. 2722–2726, IEEE, 2006. 23, 29

[61] G. R. MacCartney, J. Zhang, S. Nie, and T. S. Rappaport, "Path loss models for 5g millimeter wave propagation channels in urban microcells.," in *Globecom*, pp. 3948–3953, 2013. 23, 29

[62] A. Maltsev *et al.*, "Channel modeling and characterization-miweba," *Deliverable 5.1 EU Contract No. FP7-ICT-608637*, 2014. 23, 24, 29

[63] http://www.ieee802.org/15/pub/TG3c.html, *IEEE802.15WPAN*, 2009. 23, 24, 29

[64] T. S. Rappaport, F. Gutierrez, E. Ben-Dor, J. N. Murdock, Y. Qiao, and J. I. Tamir, "Broadband millimeter-wave propagation measurements and models using adaptive-beam antennas for outdoor urban cellular communications," *IEEE transactions on antennas and propagation*, vol. 61, no. 4, pp. 1850–1859, 2012. 23, 29

[65] K. Haneda, J. Zhang, L. Tan, G. Liu, Y. Zheng, H. Asplund, J. Li, Y. Wang, D. Steer, C. Li, *et al.*, "5g 3gpp-like channel models for outdoor urban microcellular and macrocellular environments," in *2016 IEEE 83rd Vehicular Technology Conference (VTC Spring)*, pp. 1–7, IEEE, 2016. 23, 29

[66] A. A. Saleh and R. Valenzuela, "A statistical model for indoor multipath propagation," *IEEE Journal on selected areas in communications*, vol. 5, no. 2, pp. 128–137, 1987. 23

[67] W.-. Project, *WINNER-2010*. 23

[68] T. S. Rappaport and S. Deng, "73 ghz wideband millimeter-wave foliage and ground reflection measurements and models," in *2015 IEEE International Conference on Communication Workshop (ICCW)*, pp. 1238–1243, IEEE, 2015. 23

[69] S. Hur, S. Baek, B. Kim, Y. Chang, A. F. Molisch, T. S. Rappaport, K. Haneda, and J. Park, "Proposal on millimeter-wave channel modeling for 5g cellular system," *IEEE Journal of Selected Topics in Signal Processing*, vol. 10, no. 3, pp. 454–469, 2016. 23

[70] B. Saha, E. Koshimoto, C. C. Quach, E. F. Hogge, T. H. Strom, B. L. Hill, S. L. Vazquez, and K. Goebel, "Battery health management system for electric uavs," in *2011 Aerospace Conference*, pp. 1–9, IEEE, 2011. 26

[71] I. A. Hemadeh, K. Satyanarayana, M. El-Hajjar, and L. Hanzo, "Millimeter-wave communications: physical channel models, design considerations, antenna constructions, and link-budget," *IEEE Communications Surveys & Tutorials*, vol. 20, no. 2, pp. 870–913, 2017. 26, 29

[72] P. Almers, E. Bonek, A. Burr, N. Czink, M. Debbah, V. Degli-Esposti, H. Hofstetter, P. Kyösti, D. Laurenson, G. Matz, *et al.*, "Survey of channel and radio propagation models for wireless mimo systems," *EURASIP Journal on Wireless Communications and Networking*, vol. 2007, no. 1, p. 019070, 2007. 27

[73] A. Saakian, *Radio wave propagation fundamentals*. Artech House, 2011. 28, 29

[74] 3rd Generation Partnership Project; Technical Specification Group Radio Access Network, *3GPP TR 36.814*, 2010. 32

[75] V. Aydın, İ. H. Çavdar, and Z. Hasırcı, "Line of sight (los) probability prediction for satellite and haps communication in trabzon, turkey," *International Journal of Applied Mathematics, Electronics and Computers*, no. Special Issue-1, pp. 155–160, 2016. 32

[76] Y. Yan, Q. Hu, and D. M. Blough, "Path selection with amplify and forward relays in mmwave backhaul networks," in *2018 IEEE 29th Annual International Symposium on Personal, Indoor and Mobile Radio Communications (PIMRC)*, pp. 1–6, IEEE, 2018. 36

[77] T. Q. Duong, L.-N. Hoang, and V. N. Q. Bao, "On the performance of two-way amplify-and-forward relay networks," *IEICE transactions on communications*, vol. 92, no. 12, pp. 3957–3959, 2009. 36

[78] O. Bello, H. Zen, A.-K. Othman, and K. A. Hamid, "Computing amplify-and-forward relay amplification factor to improve total capacity at destination," *American Journal of Applied Sciences*, vol. 12, no. 8, p. 572, 2015. 36

[79] R. Viswanathan, "Signal-to-noise ratio comparison of amplify-forward and direct link in wireless sensor networks," in *2007 2nd International Conference on Communication Systems Software and Middleware*, pp. 1–4, IEEE, 2007. 36, 37

[80] D. Roddy, *Satellite communications*. McGraw-Hill Prof Med/Tech, 2006. 36, 37

[81] J. B. Schodorf, "Land-mobile satellite communications," *Wiley Encyclopedia of Telecommunications*, 2003. 37

[82] Z. Yun and M. F. Iskander, "Ray tracing for radio propagation modeling: Principles and applications," *IEEE Access*, vol. 3, pp. 1089–1100, 2015. 40

[83] L. Subrt and P. Pechac, "Advanced 3d indoor propagation model: calibration and implementation," *EURASIP Journal on Wireless Communications and Networking*, vol. 2011, no. 1, p. 180, 2011. 40, 41

[84] https://www.remcom.com/wireless-insite-em-propagation-softwarewireless-insite-em-propagation features, *Wireless InSIte*, https://www.remcom.com/wireless-insite-em-propagation-softwarewireless-insite-em-propagation-features. 40, 41

[85] . Evolved Universal Terrestrial Radio Access, *Evolved Universal Terrestrial Radio Access*, https://www.etsi.org. 41, 46, 51

[86] https://www.etsi.org/deliver/etsi$_t r$/136900$_1$36999/136942/13.00.00$_6$0/$tr_1$36942v130000$p.pdf$, $3GPPTR36.9TECHN$

[87] ITU, *ETSI 3rd Generation Partnership Project (3GPP)*, 2009. 51

[88] M. Foegelle, "Creating a complex multipath environment simulation in an anechoic chamber," *Microwave Journal*, vol. 53, 08 2010. 53

[89] www.sharetechnote.com, *5G - FD MIMO*, 2018. 53

[90] Ericson, "Ericson technical report, https://www.ericsson.com/assets//mobility-report/documents/2018/ericsson-mobility-report-june-2018.pdf."

[91] Austrilia, *Drone Laws Aus*, https://www.rpastraining.com.au/drone-laws.

[92] H. Zhao, R. Mayzus, S. Sun, M. Samimi, J. K. Schulz, Y. Azar, K. Wang, G. N. Wong, F. Gutierrez, and T. S. Rappaport, "28 ghz millimeter wave cellular communication measurements for reflection and penetration loss in and around buildings in new york city," in *2013 IEEE International Conference on Communications (ICC)*, pp. 5163–5167, June 2013.

[93] A. K. M. Baki, M. W. Absar, T. Rahman, and K. M. A. Ahamed, "Investigation of rayleigh and rician fading channels for state of the art (soa) lte-ofdm communication system," in *2017 4th International Conference on Advances in Electrical Engineering (ICAEE)*, Sep. 2017.

[94] Marketinsightsreports, *Market insights reports*, 2017.

[95] 3GPP, *Study on channel model for frequencies from 0.5 to 100 GHz (3GPP TR 38.901 version 14.3.0 Release 14)*, 2018.

[96] L. Xie, J. Xu, and R. Zhang, "Throughput maximization for uav-enabled wireless powered communication networks," *IEEE Internet of Things Journal*, 2018.

[97] S. Hur, T. Kim, D. J. Love, J. V. Krogmeier, T. A. Thomas, and A. Ghosh, "Millimeter wave beamforming for wireless backhaul and access in small cell networks," *IEEE transactions on communications*, vol. 61, no. 10, pp. 4391–4403, 2013.

[98] D. Senaratne and C. Tellambura, "Unified exact performance analysis of two-hop amplify-and-forward relaying in nakagami fading," *IEEE Transactions on Vehicular Technology*, vol. 59, no. 3, pp. 1529–1534, 2009.

[99] J. Lyu, Y. Zeng, R. Zhang, and T. J. Lim, "Placement optimization of uav-mounted mobile base stations," *IEEE Communications Letters*, vol. 21, no. 3, pp. 604–607, 2016.

[100] F. Ono, H. Ochiai, and R. Miura, "A wireless relay network based on unmanned aircraft system with rate optimization," *IEEE Transactions on Wireless Communications*, vol. 15, pp. 7699–7708, Nov 2016.

[101] E. Larsen, L. Landmark, and Kure, "Optimal uav relay positions in multi-rate networks," in *2017 Wireless Days*, pp. 8–14, March 2017.

[102] Z. Dejin, Y. Ning, W. Liaoni, and Z. Shenglu, "A kind of moving net recovery technology for unmanned aerial vehicle," 2015.

[103] J. Dong, Q. Chen, and Z. Niu, "Random graph theory based connectivity analysis in wireless sensor networks with rayleigh fading channels," in *2007 Asia-Pacific Conference on Communications*, pp. 123–126, IEEE, 2007.

[104] S. Rohde and C. Wietfeld, "Interference aware positioning of aerial relays for cell overload and outage compensation," in *2012 IEEE vehicular technology conference (VTC Fall)*, pp. 1–5, IEEE, 2012.

[105] I. Bor-Yaliniz and H. Yanikomeroglu, "The new frontier in ran heterogeneity: Multi-tier drone-cells," *IEEE Communications Magazine*, vol. 54, no. 11, pp. 48–55, 2016.

[106] Q. Chen, X. Wang, and Y. Lv, "An overview of 5g network slicing architecture," in *AIP Conference Proceedings*, vol. 1967, p. 020004, AIP Publishing, 2018.